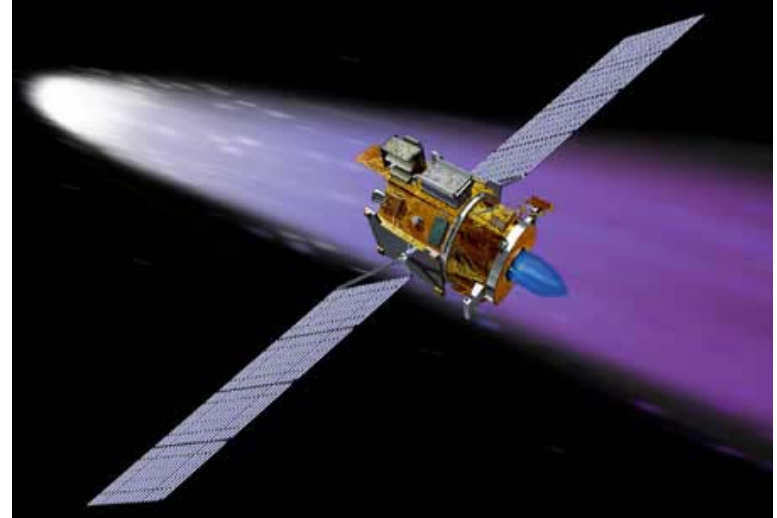


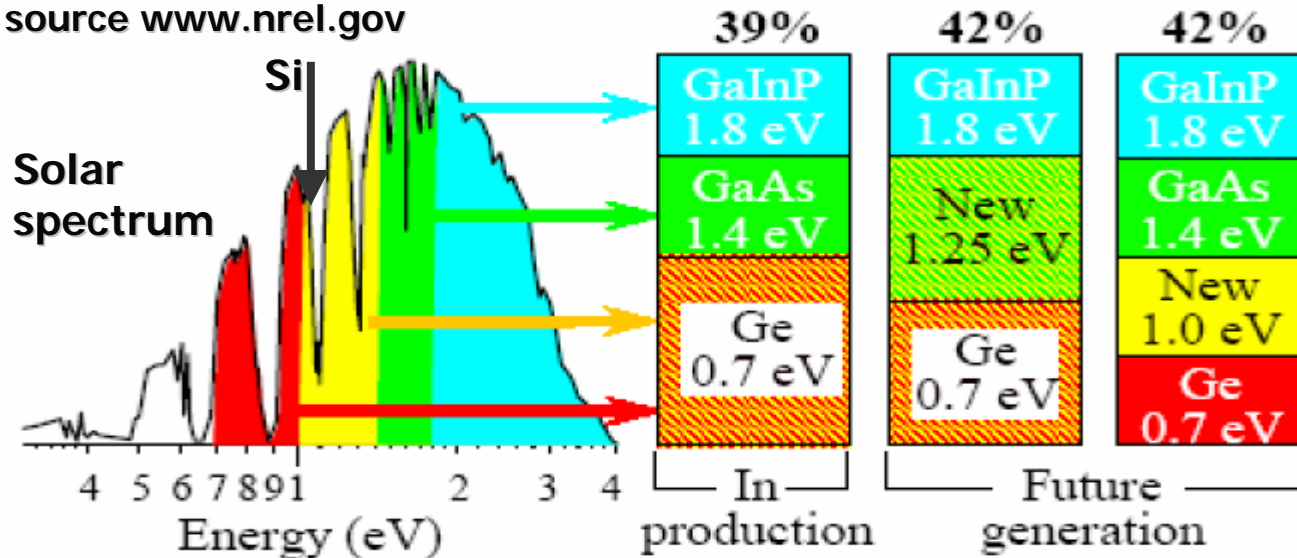
Simulation of multi-junction compound solar cells

Introduction

- Multi-junction (MJ) solar cells – space (e.g. NASA Deep Space 1) & terrestrial applications.
- More efficient & better radiation hardness.
- More sensitive to illumination spectra change.



source www.nrel.gov



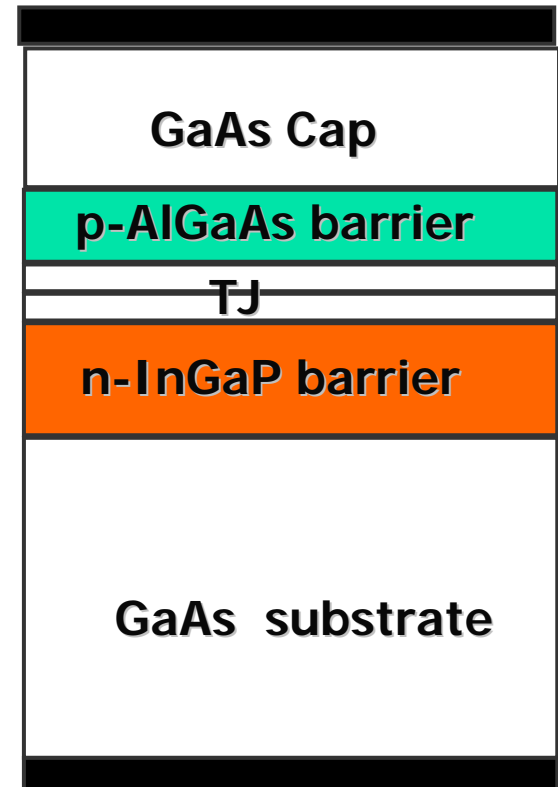
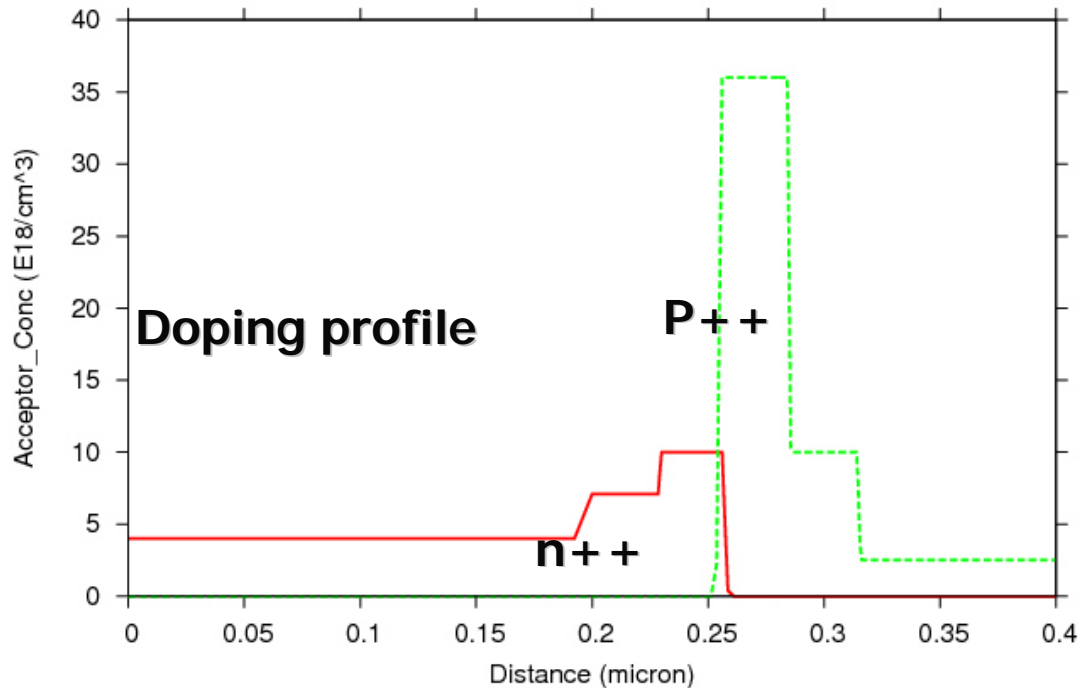
Introduction

- **Compound solar cells have many layers with different composition, thickness and doping density, need to be optimized.**
- **Better methods & software, especially with 2D/3D modeling capability in high demand.**
- **Save R&D time/cost & capability in optimizing device design. Better understanding & predicting the operation condition.**
- **In this work, based on drift-diffusion theory & Crosslight's APSYS, single, dual and triple junction solar cells are simulated and compared with experiments.**

APSYS models related to solar cells

- Non-local quantum tunneling (intra- & inter-band) model – tunneling junctions.
- All physical processes – carrier generation, recombination, drift & diffusion with 2D/3D modeling capability.
- Self-heating, series resistance, shadowing, and edge effects can be included.
- Multi-layer optics model – internal reflections & interferences.
- FDTD and Ray-tracing (RT) for edge effect & for cell with texture.
- Comprehensive material database for compound semiconductors

Tunnel Junction



Prog. Photov. Res. & Appl., 2008

Non-local Tunneling Model

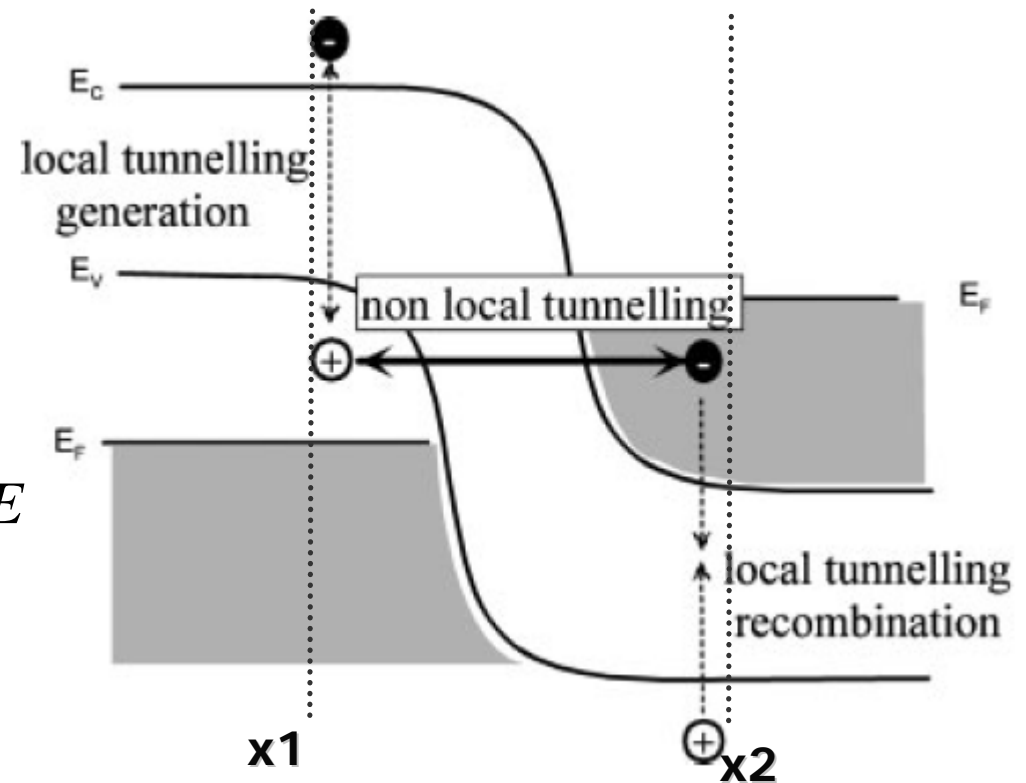
Based on WKB approx. tunneling probability

Tunneling probability:

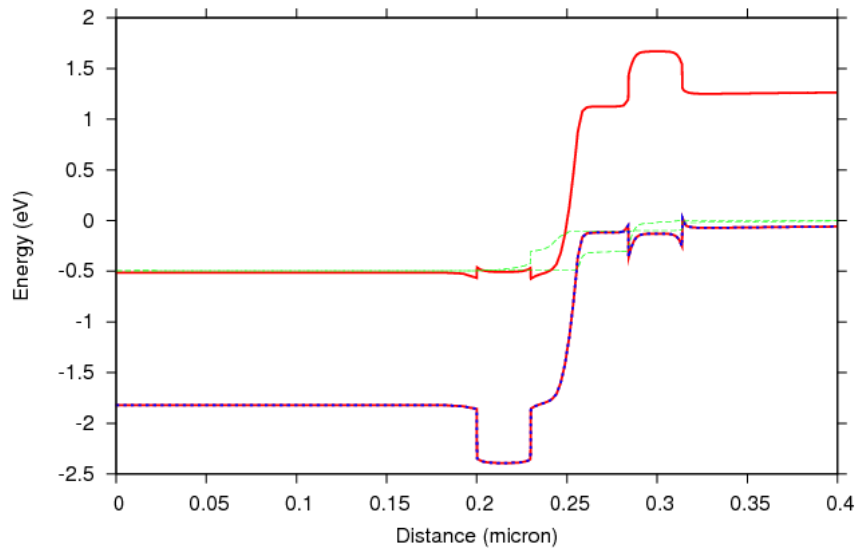
$$D = \exp\left(-2 \int_{x_1}^{x_2} |k(x)| dx\right)$$

Tunneling current:

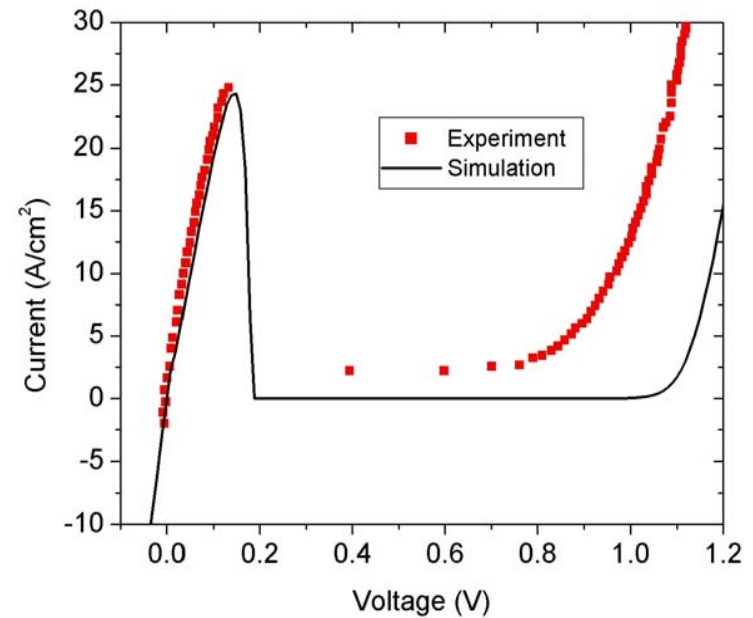
$$J_t = \int_{E_c}^{E_v} (F_c - F_v) D n_c(E) n_v(E) dE$$



I-V of Tunnel Junction



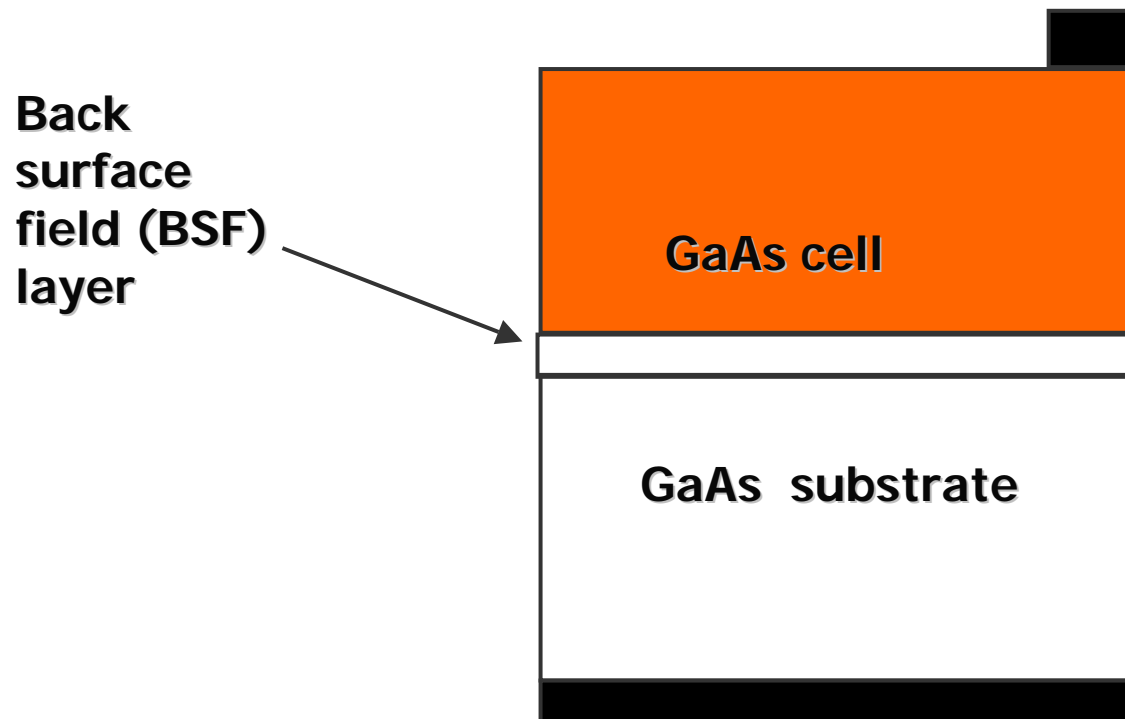
Band diagram at 0.5V reverse bias



Prog. Photov. Res. & Appl., 2008

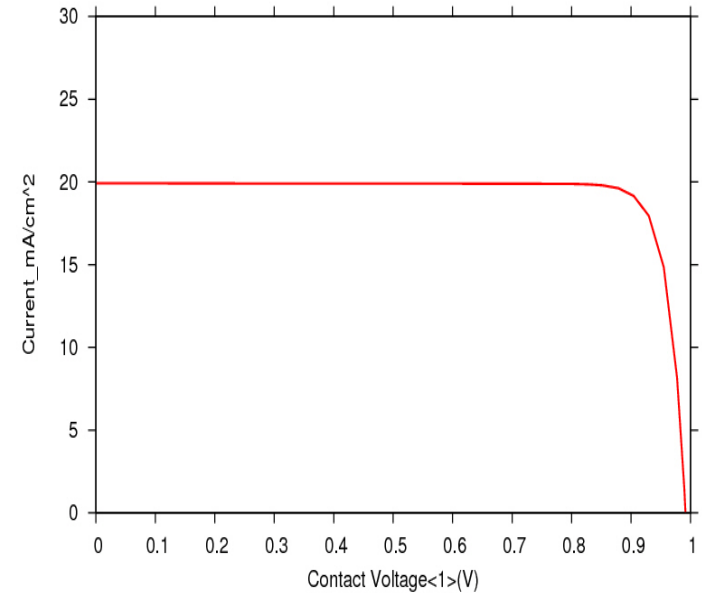
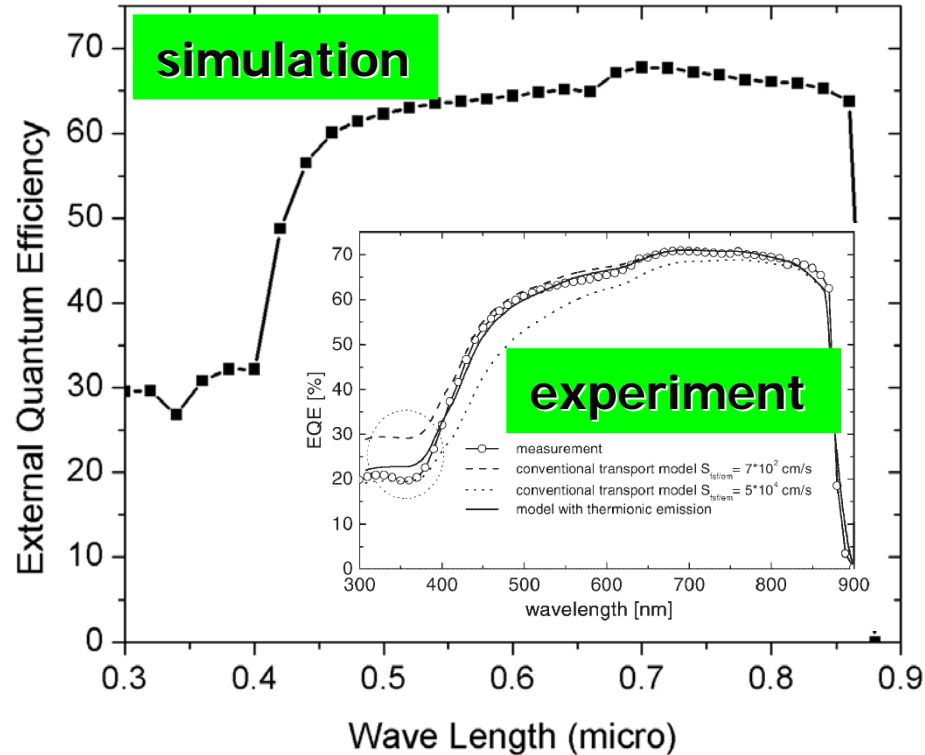
GaAs Solar Cell

Note: no window and AFC layers



Progs. Photov. Res. & Appl. Vol.14, p. 683, 2006

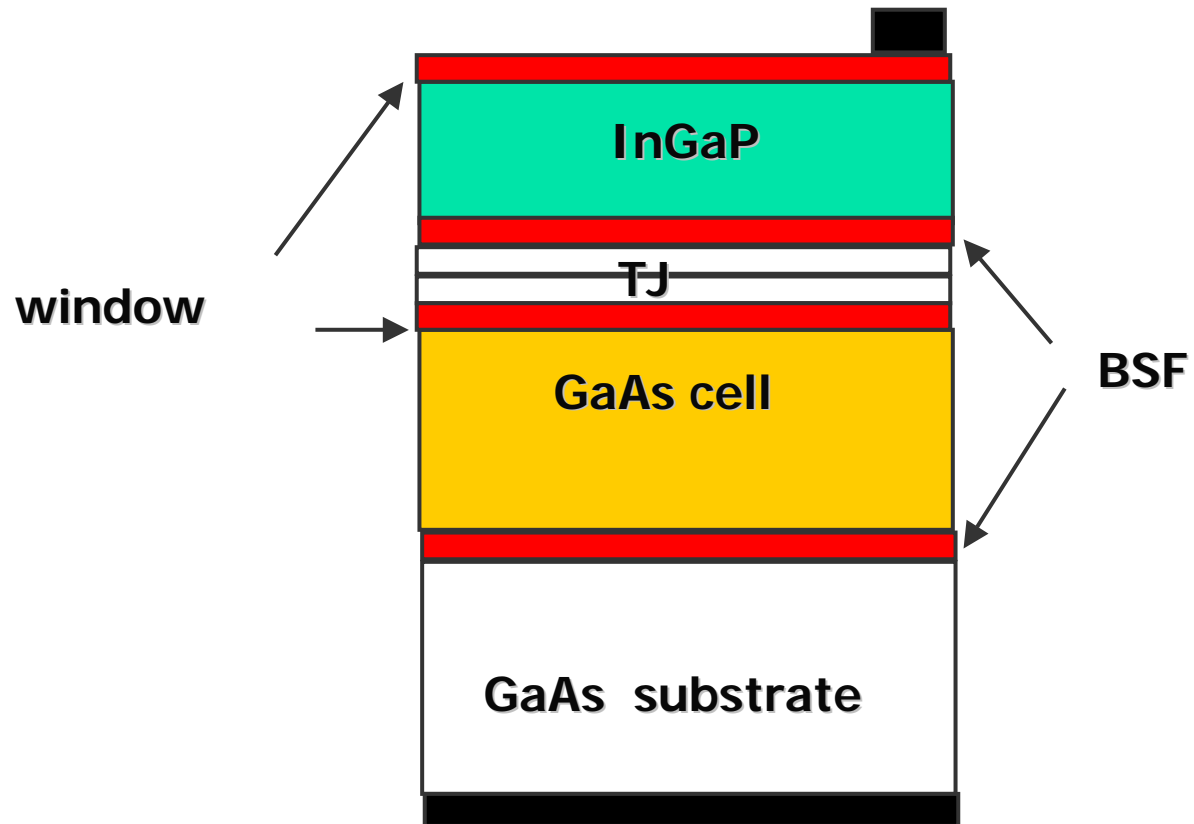
EQE and I-V



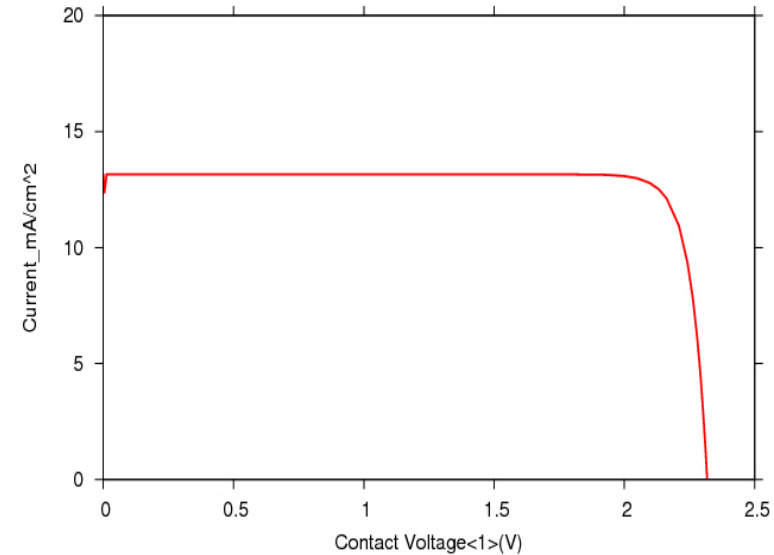
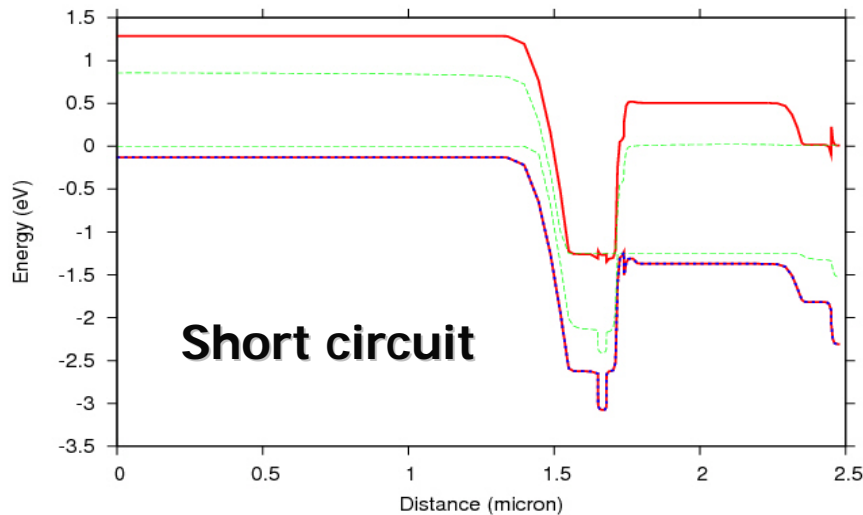
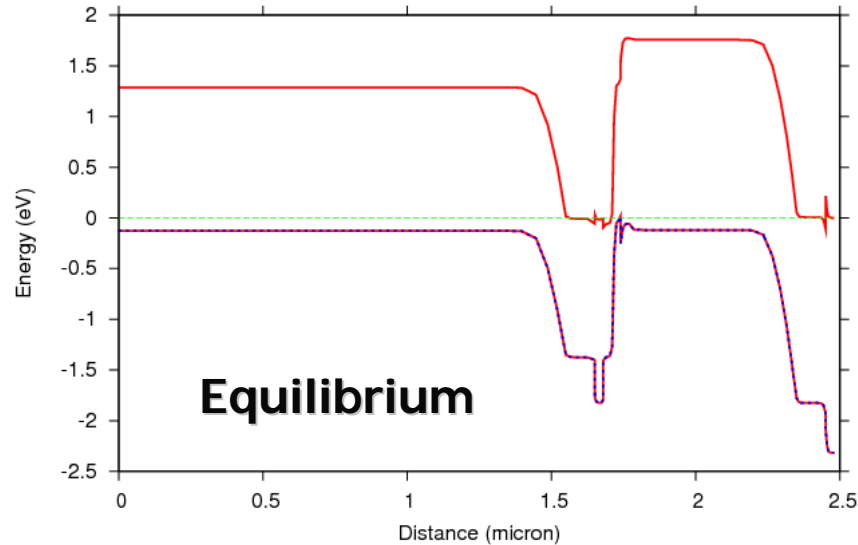
Progs. Photov. Res. & Appl. Vol. 14,
p. 683, 2006

	Jsc	Voc
Simulation	19.92	0.991
Exp	19.3	0.991

Dual-Junction

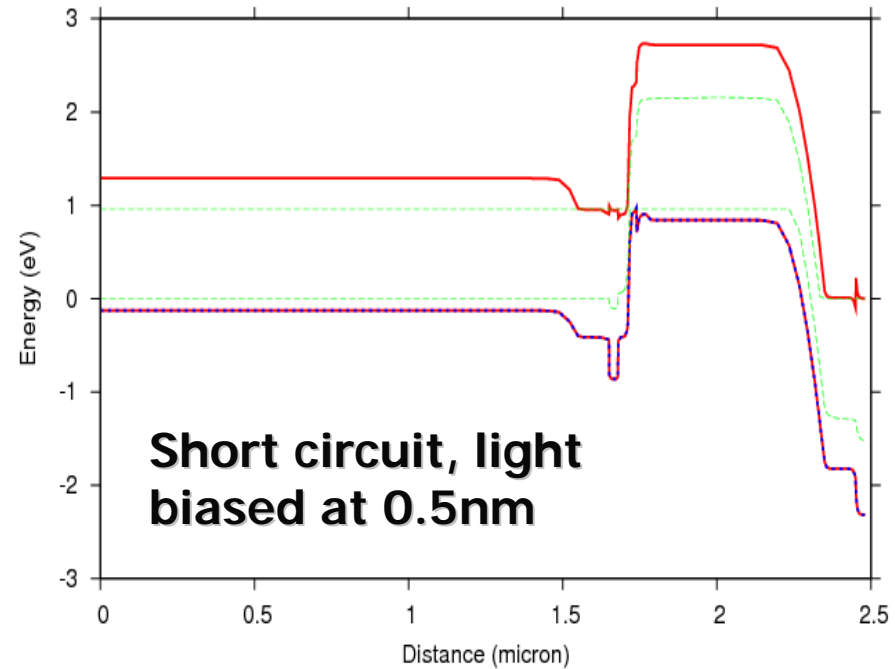
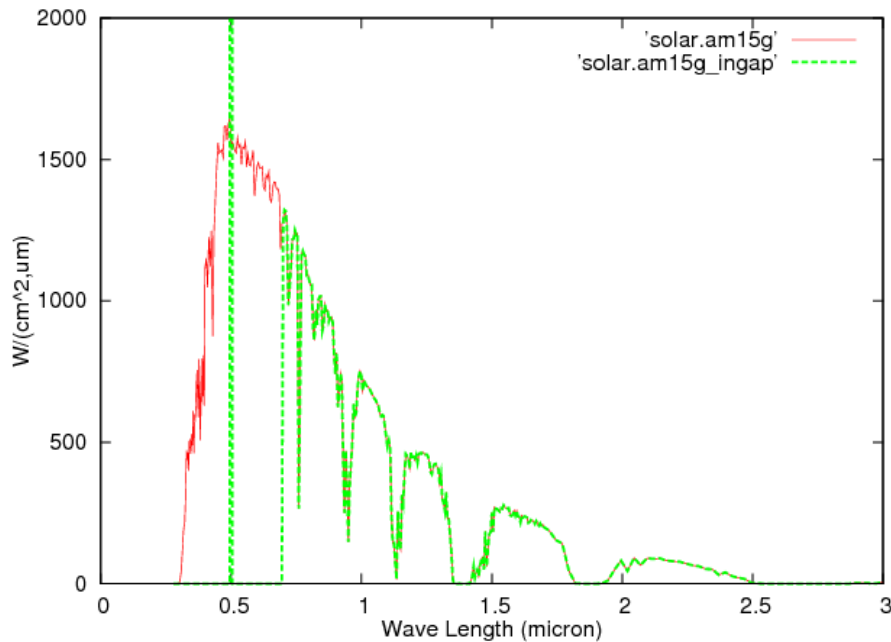


Band Diagrams and I-V



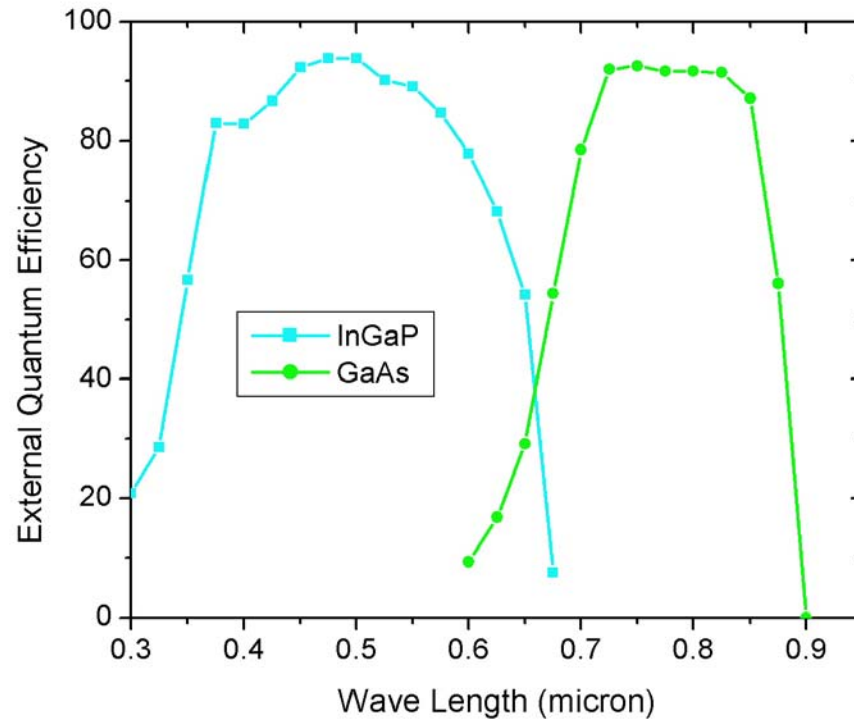
Band diagram at equilibrium (top) and short circuit (bottom), showing GaAs cell is current limiting, since it is reverse biased.

EQE Calculation

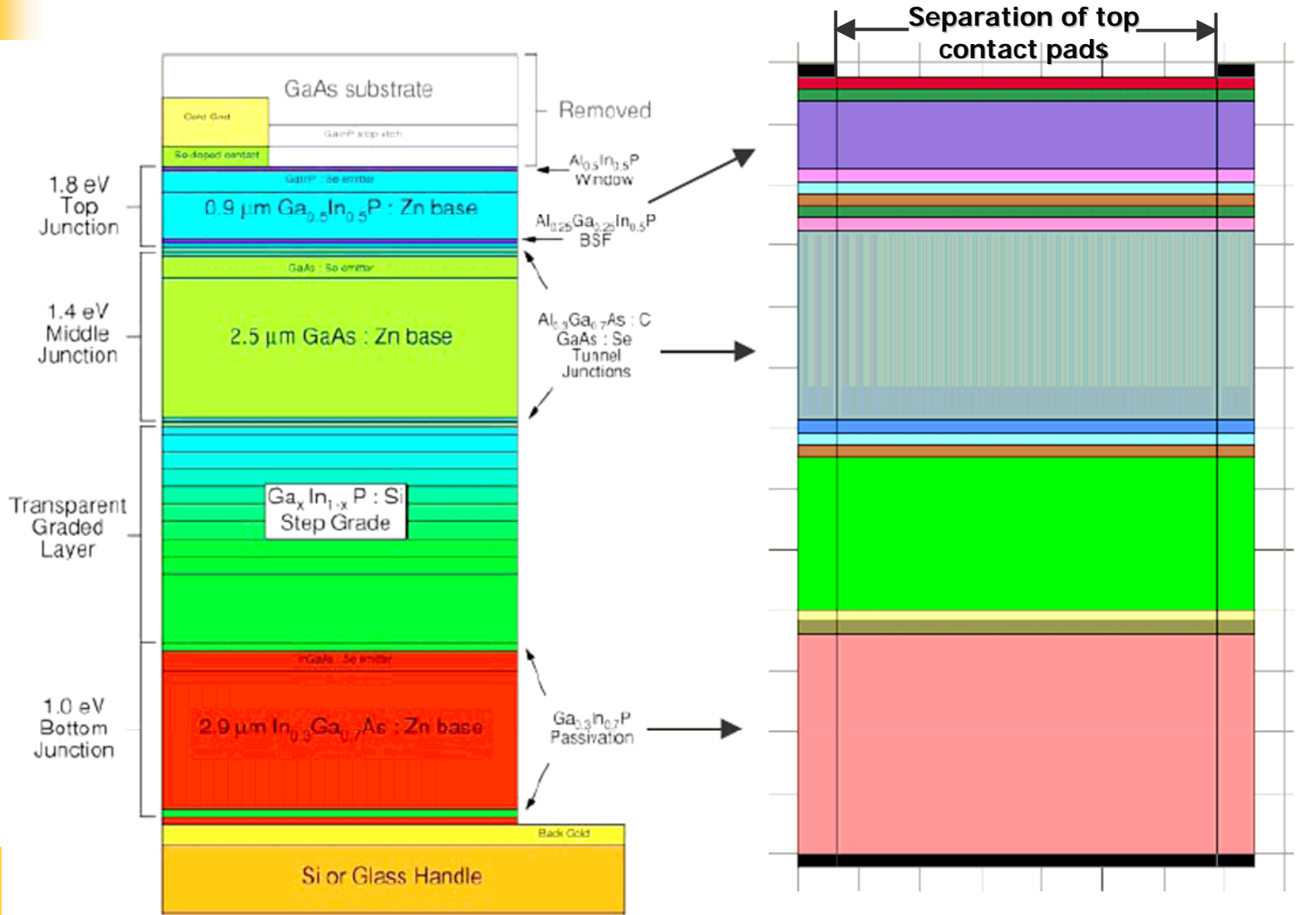


Light power for target sub-cell is filtered, with only 100 w/m^2 light bias at target wave length, so the target sub-cell is current limiting (reverse biased).

EQE of Dual-Junction Cell



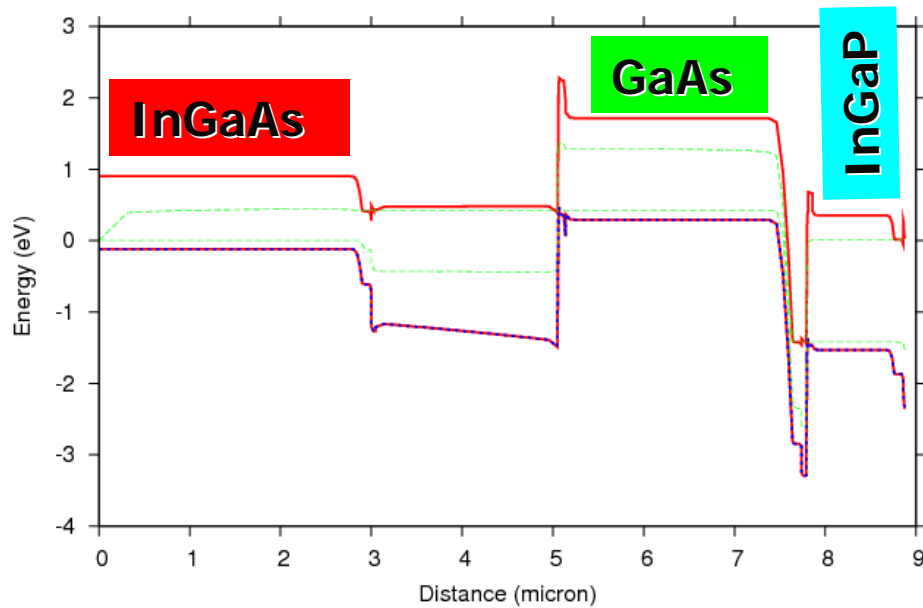
Inverted Triple-Junction



Geisz et al, APL 91, 023502 (2007)

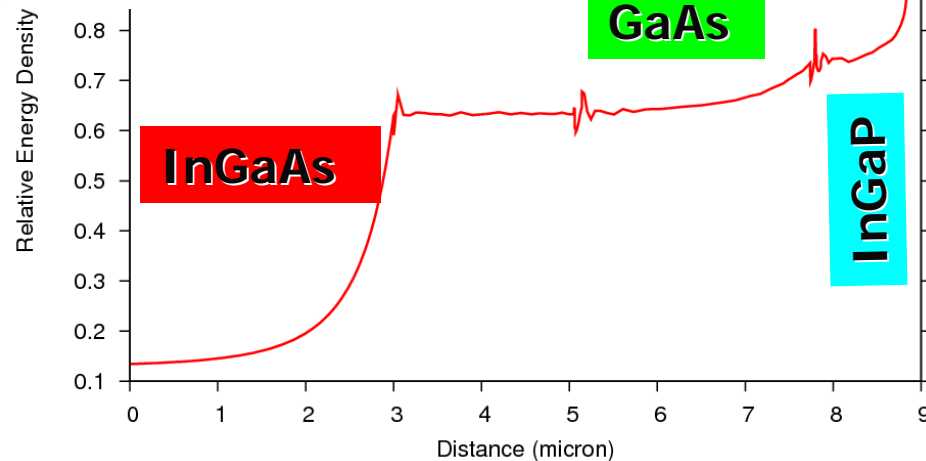
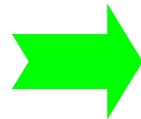
CROSSLIGHT
Software Inc.

Band Diagrams & Optical Generation

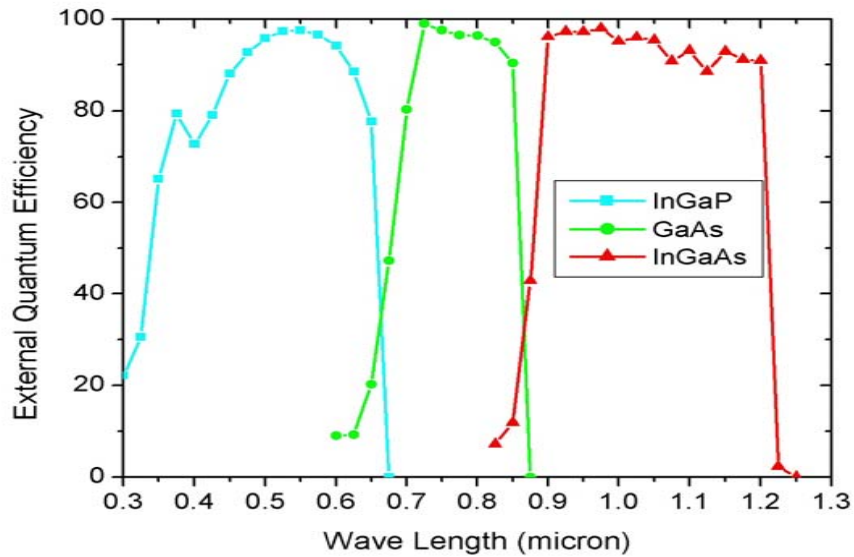


Band diagram at short circuit. GaAs is current limiting cell, which is at high reverse bias.

Relative incident power.



External Quantum Efficiency



↑
Simulated

Geisz et al, APL 91, 023502 (2007)

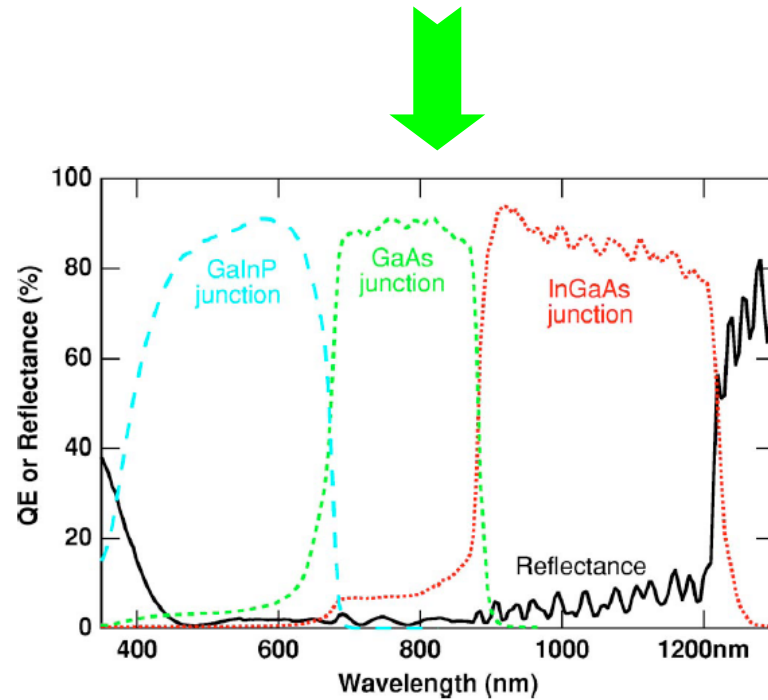
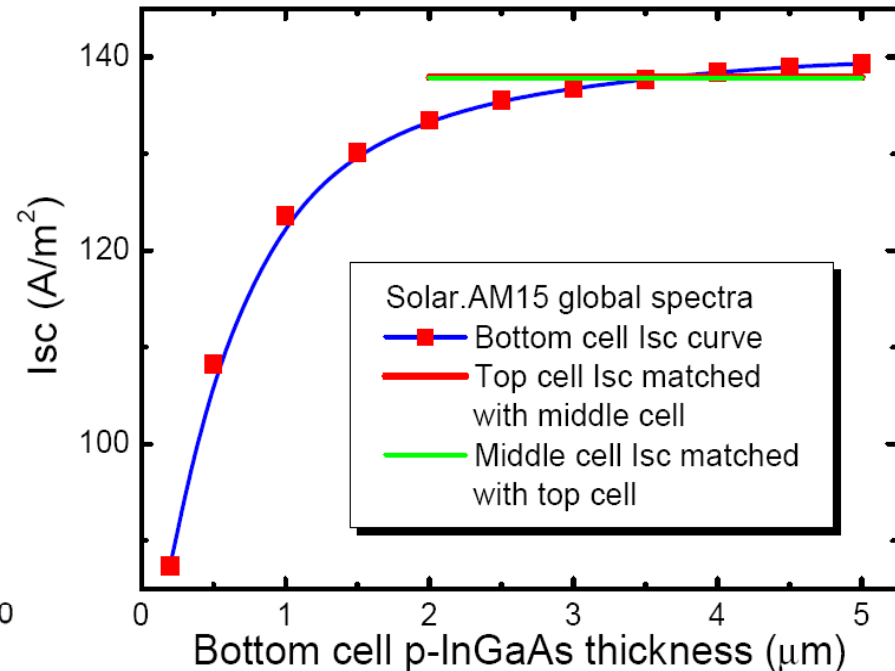
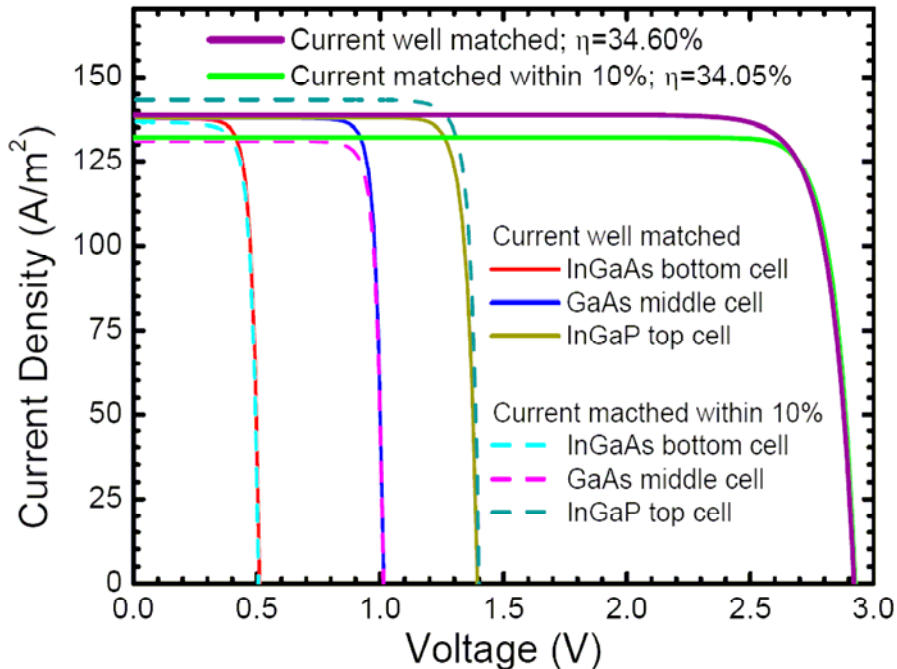


FIG. 3. External quantum efficiency and specular reflectance of the AM1.5G inverted triple-junction device.

I-V Curves: Current Matching

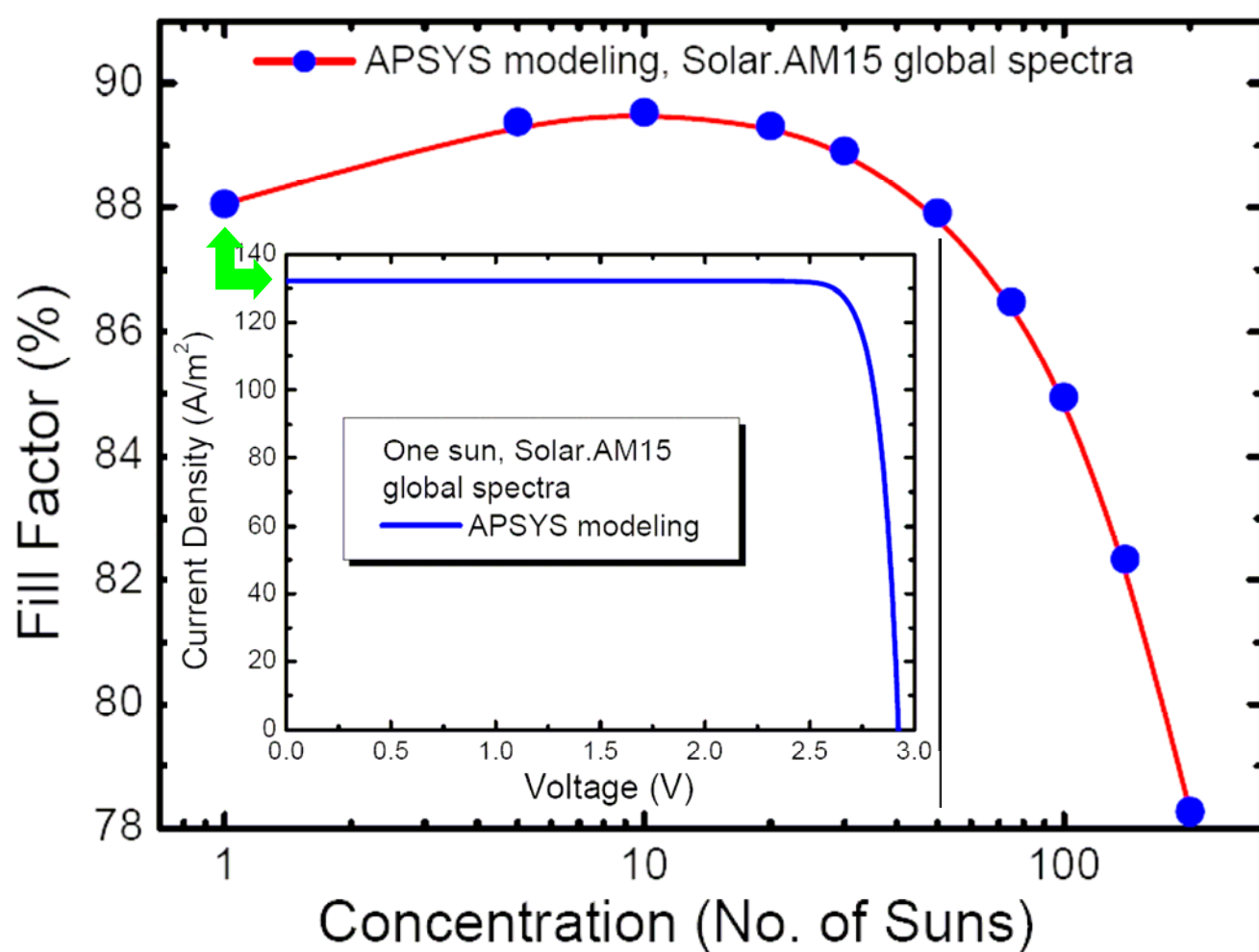


	Voc (V)	Isc (mA/cm^2)	Efficiency (%)
Experimental	2.96	13.1	33.8
Modeling	2.93	13.2	34.1

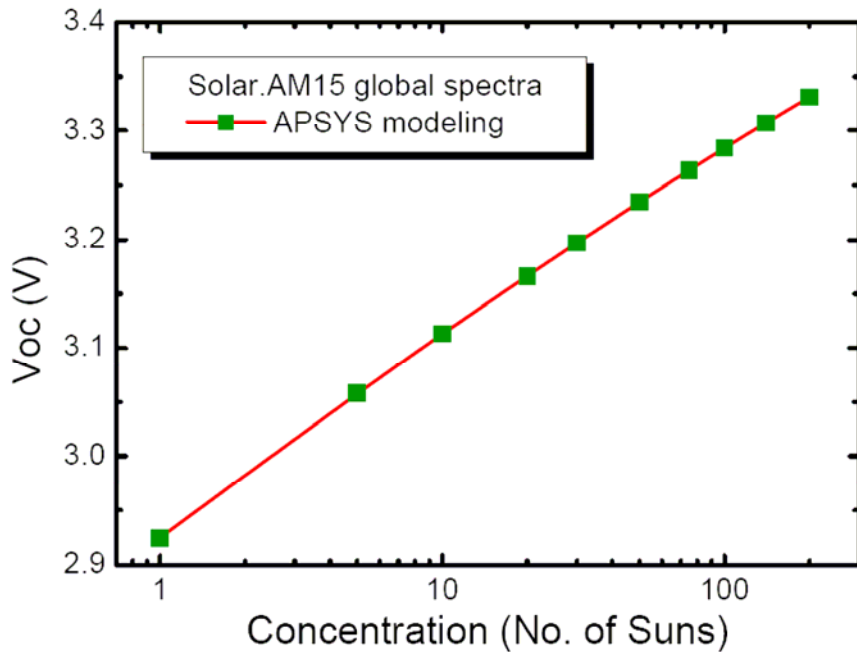
← Comparing the case when current matched within 10%.

- Conversion efficiency improved when current matched with middle & top subcells.
- Modeling results of Voc, Isc & efficiency comparable with experimental results.

Multi-Sun Concentration: Fill Factor

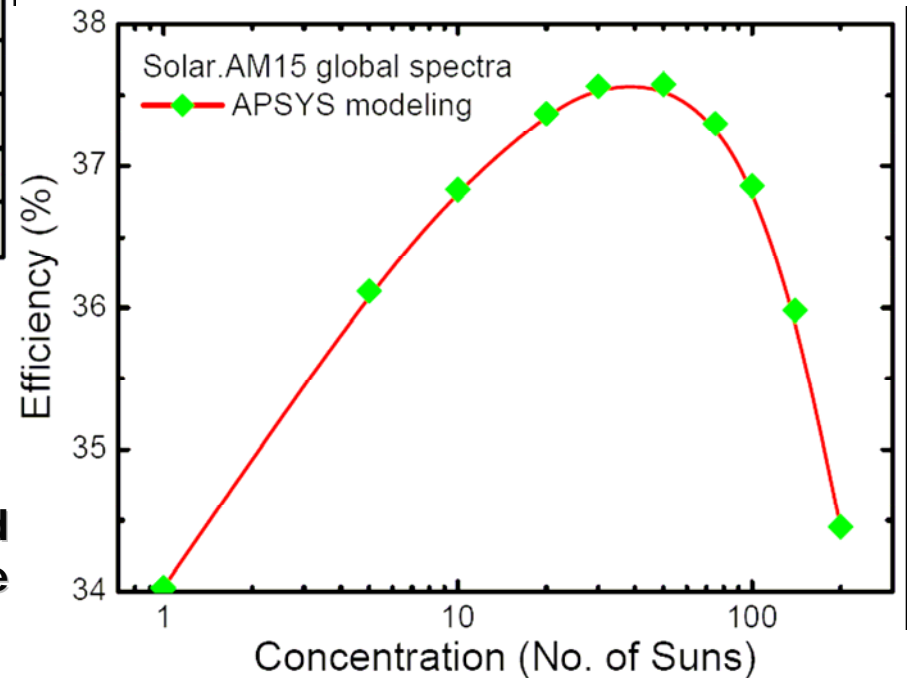


Multi-Sun Concentration: Voc & Efficiency

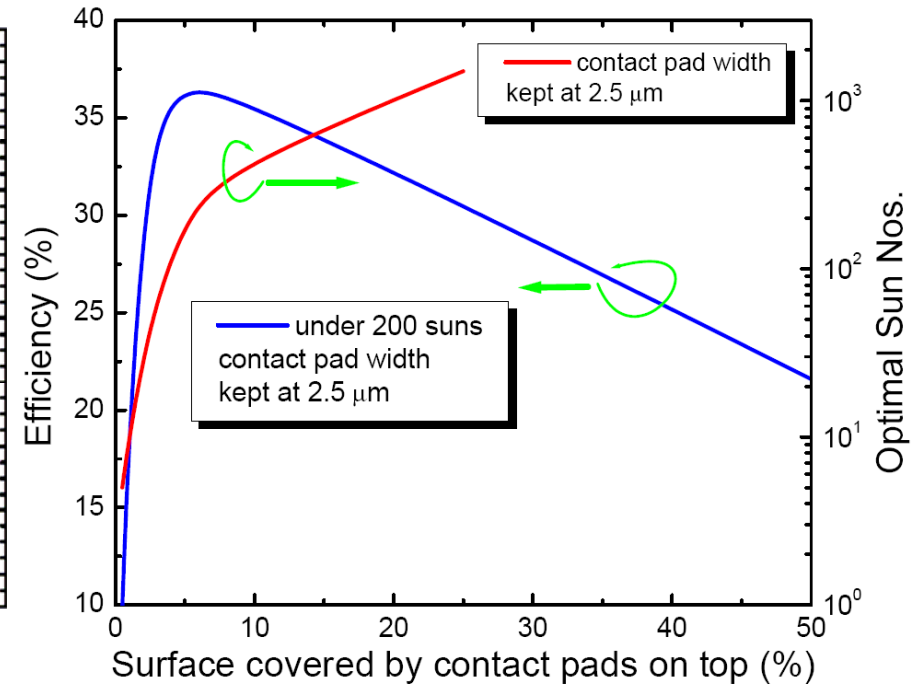
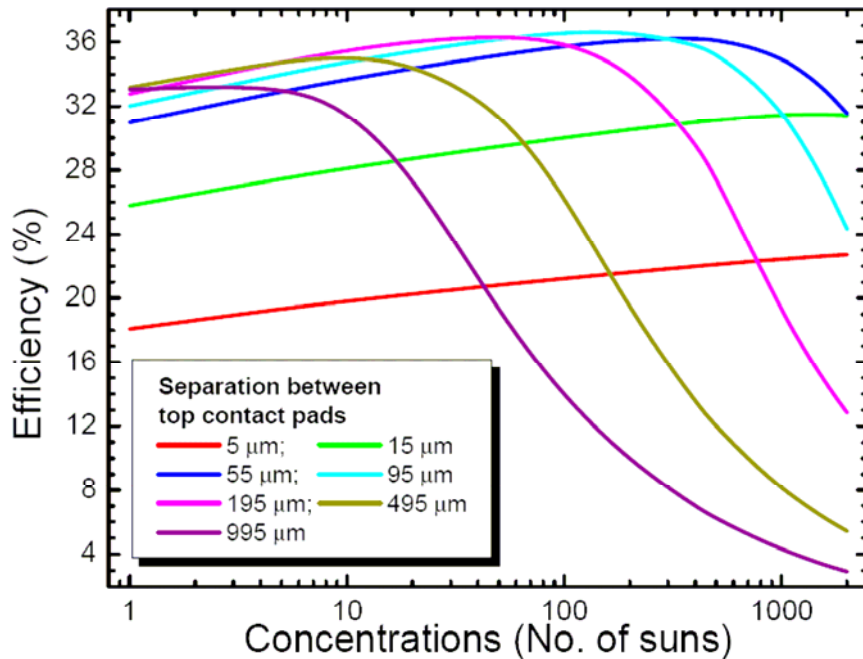


V_{oc} is logarithmically proportional with concentration.

Cell efficiency enhanced versus sun No. initially due to enhanced V_{oc} . Afterwards it decreases due to series resistance.



Multi-Sun Concentration: Efficiency



- Optimal sun number varies with contact pad separation, indicating different series resistance effect.
- At fixed sun number, optimal efficiency appears at certain top contact pad separation where a specific ratio covered by top contact pads is identified.

3D InGaP/GaAs/Ge TJ Solar Cell Structure

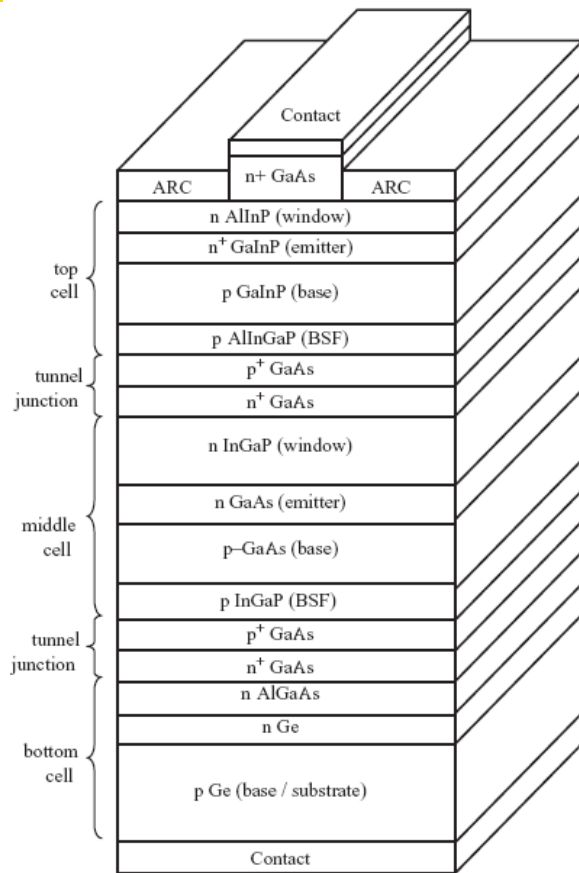
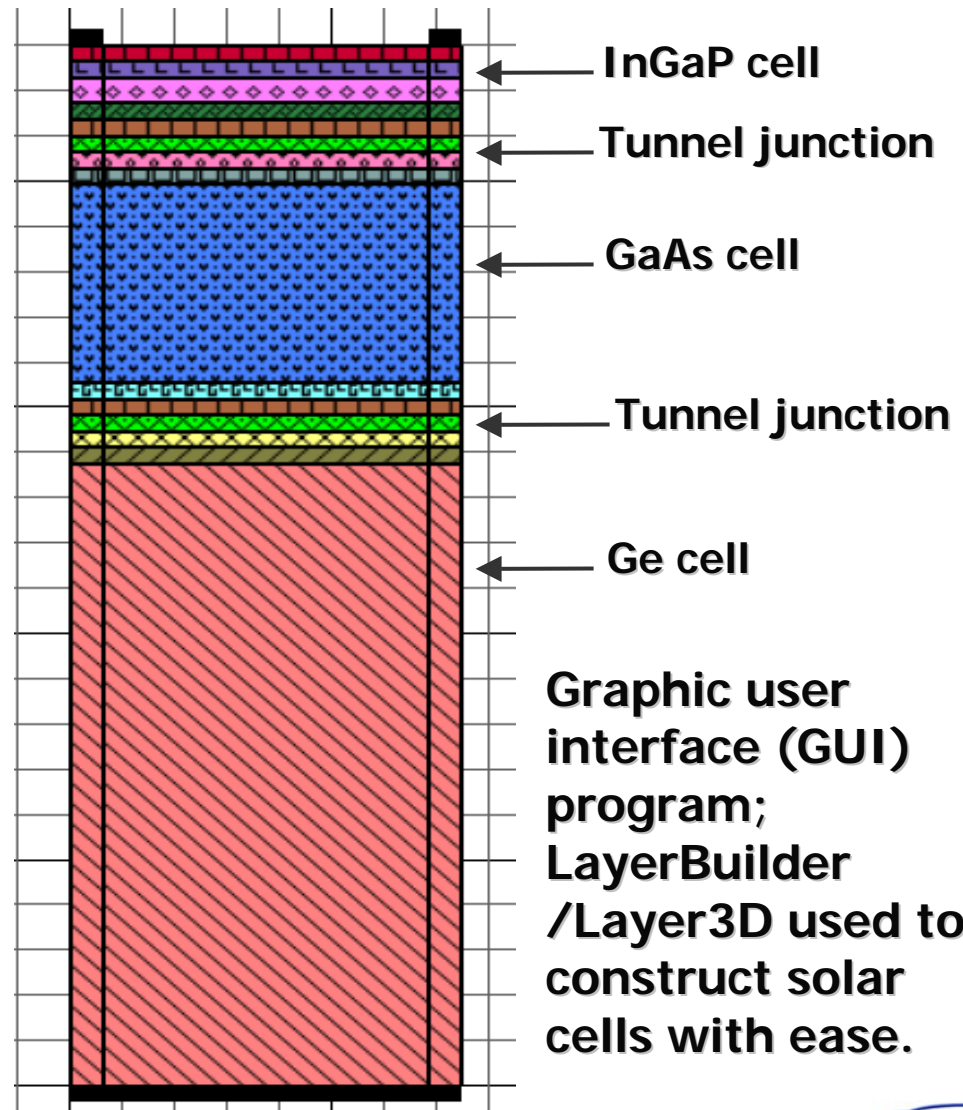
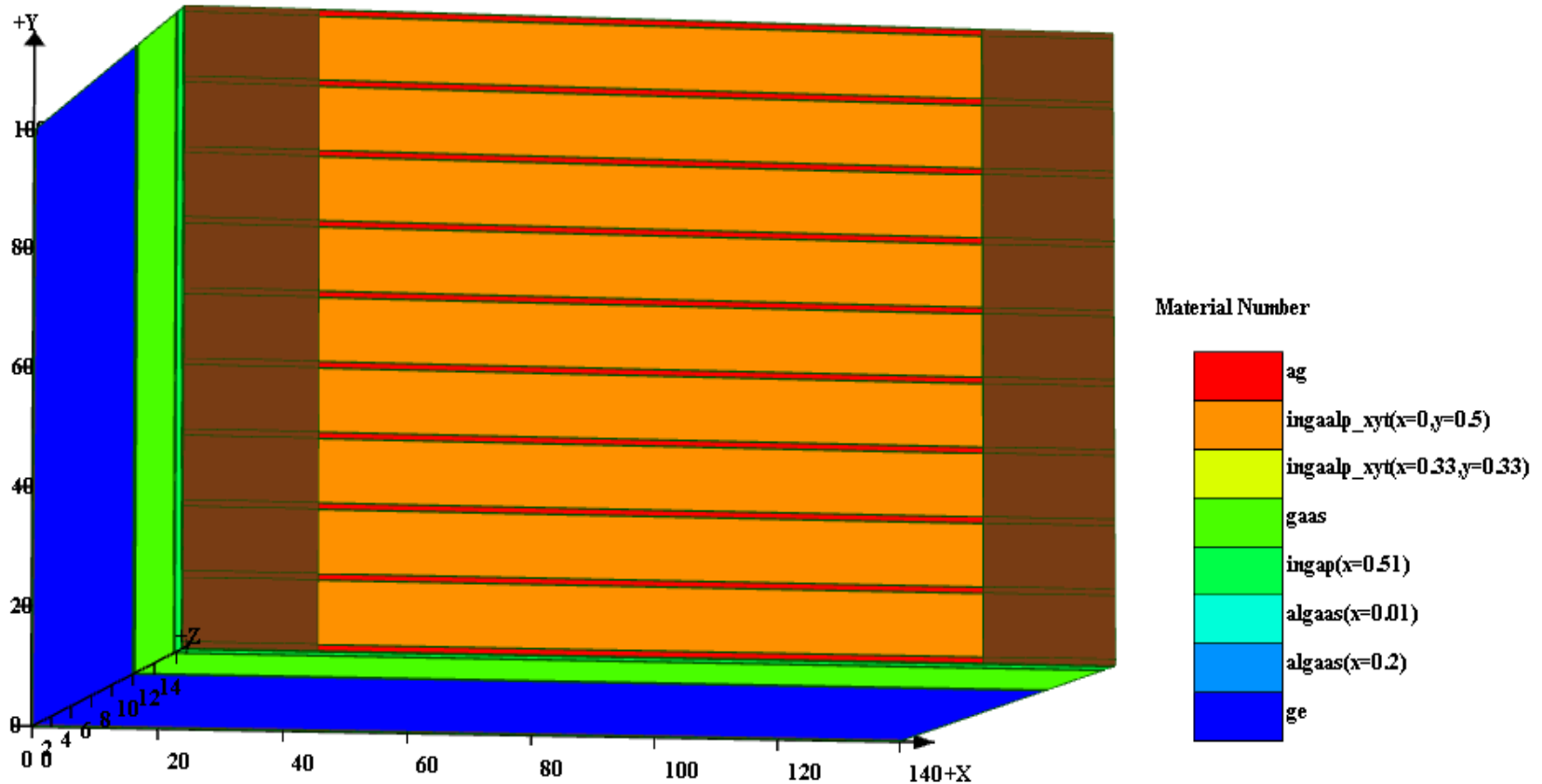


Fig. 9. 3D layout of the triple-junction model.

IEEE Trans. Elec. Devices,
v. 46, p. 2116, 1999

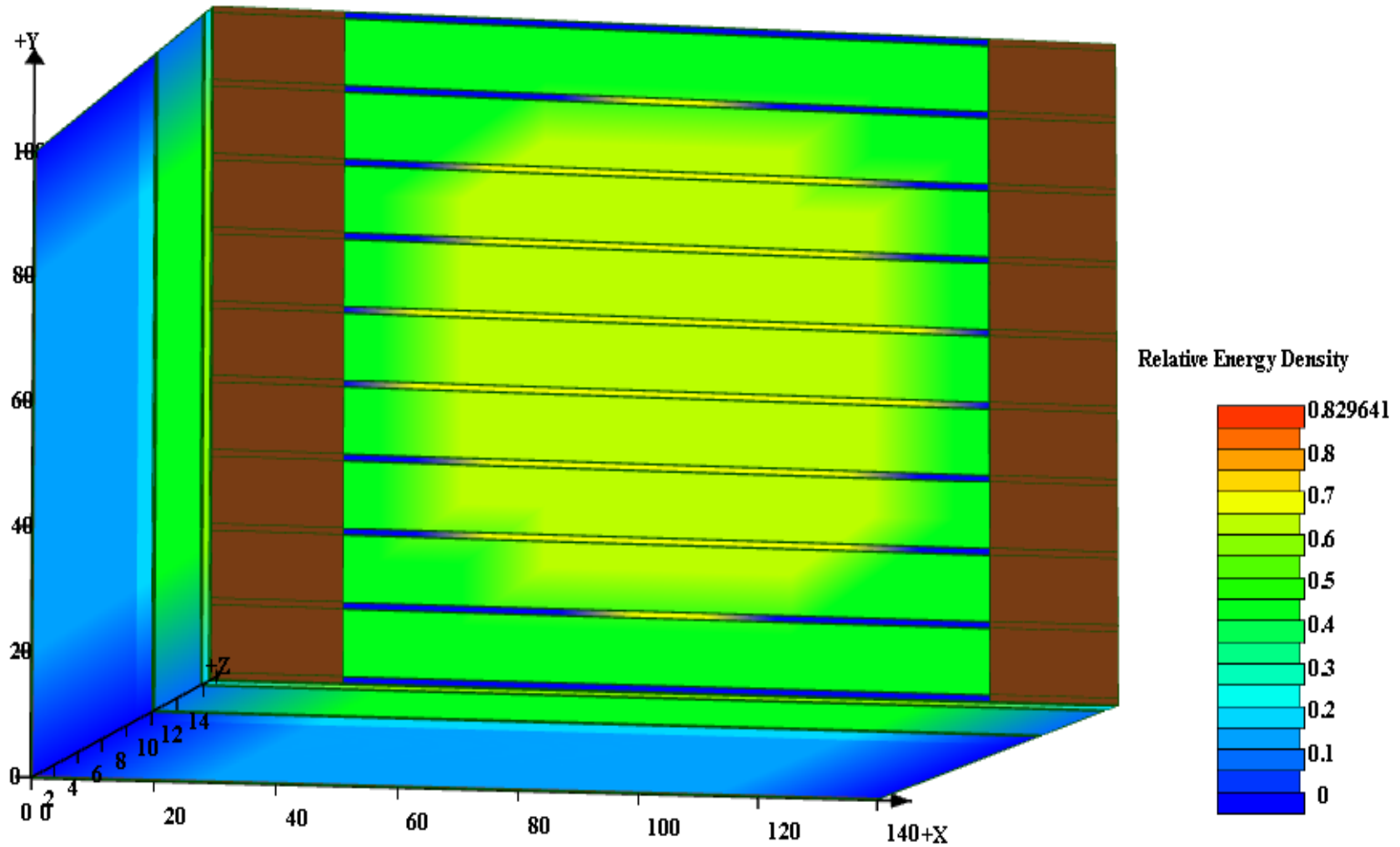


3D Material/Layer Structure



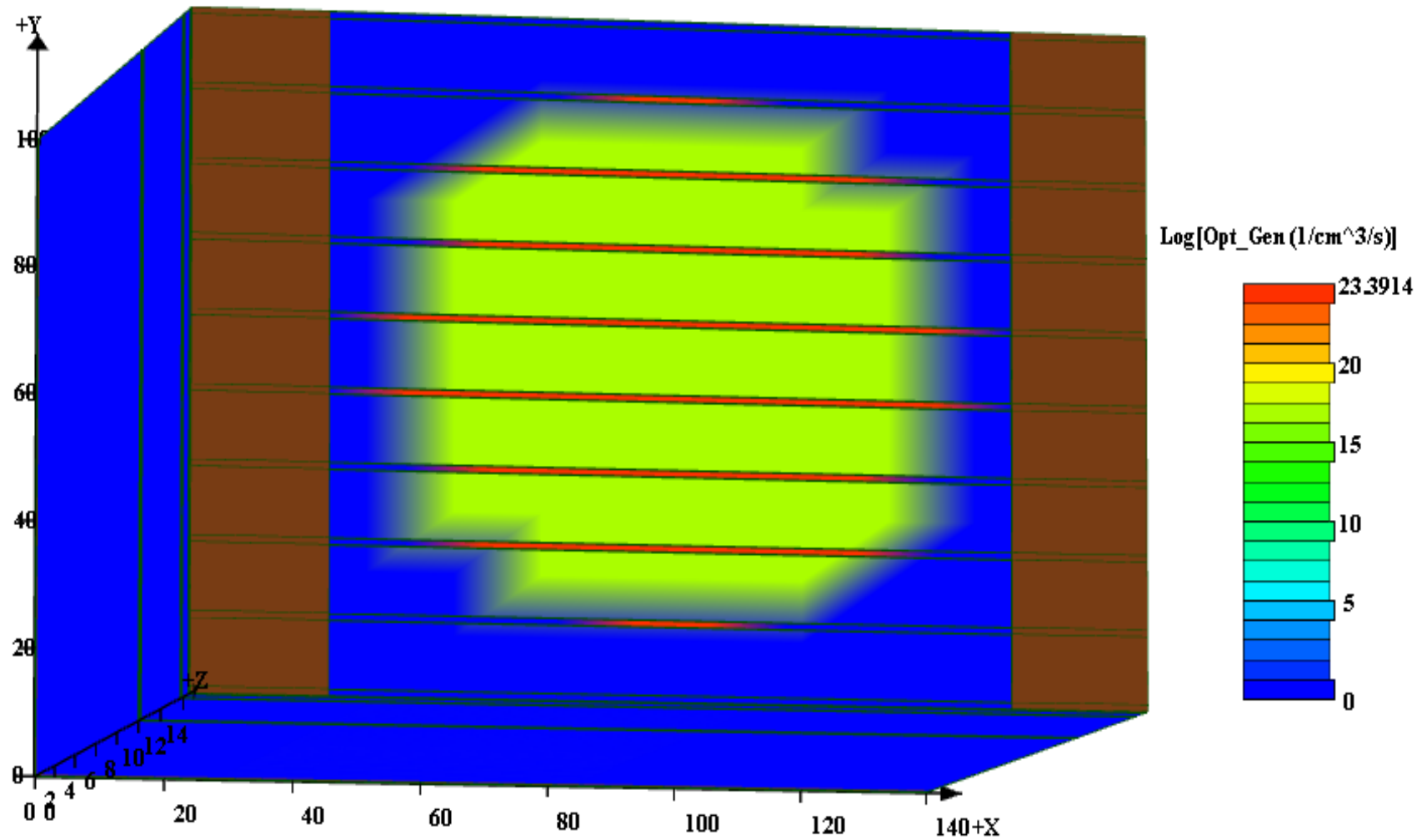
3D simulation results courtesy of C.K. Chao (INER - Taiwan)
and J.J. Guo (Grand Technology Inc. - Taiwan)

3D incident_power

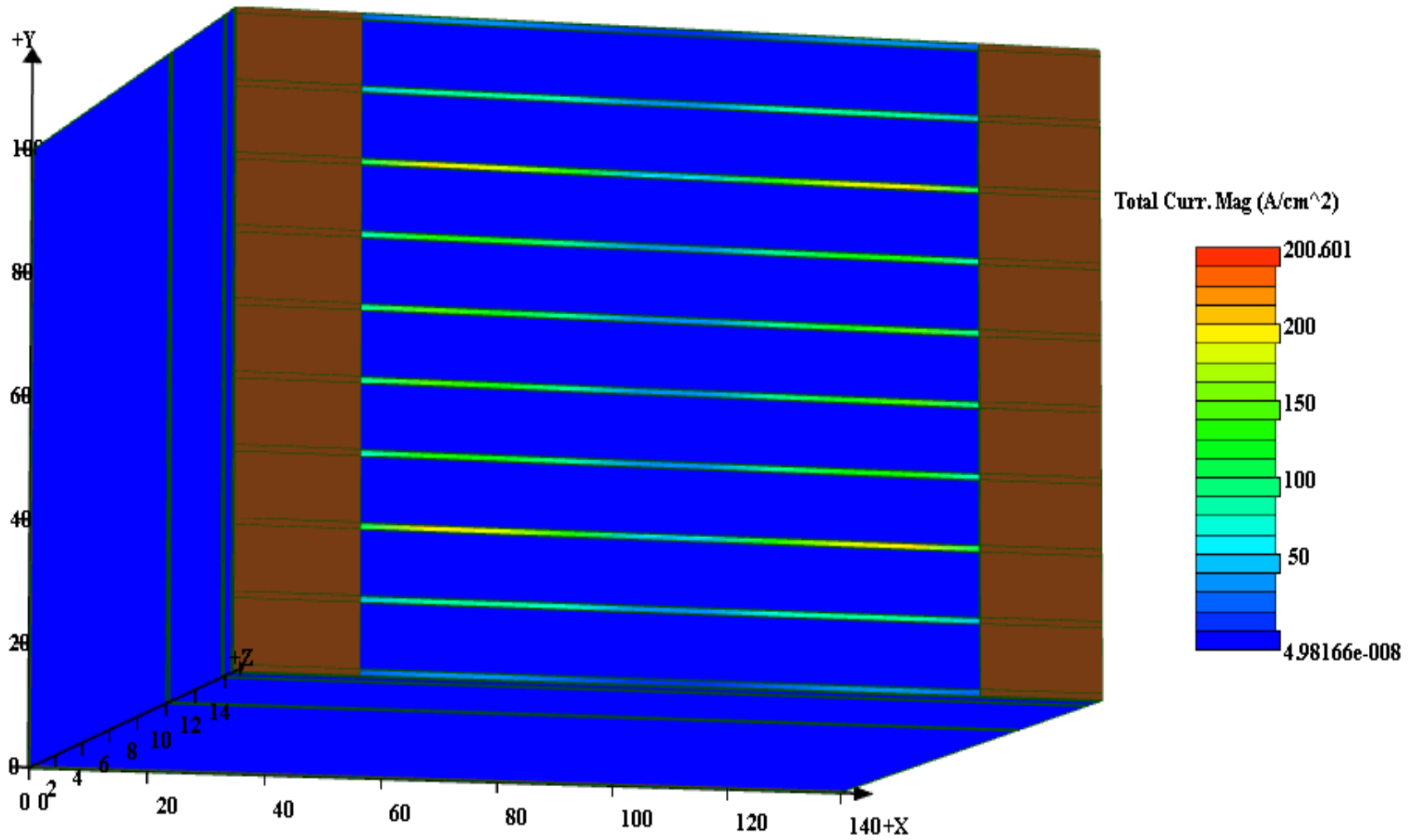


Simulated for Focused beam incident on center of top area.

3D Optical Absorption/Generation

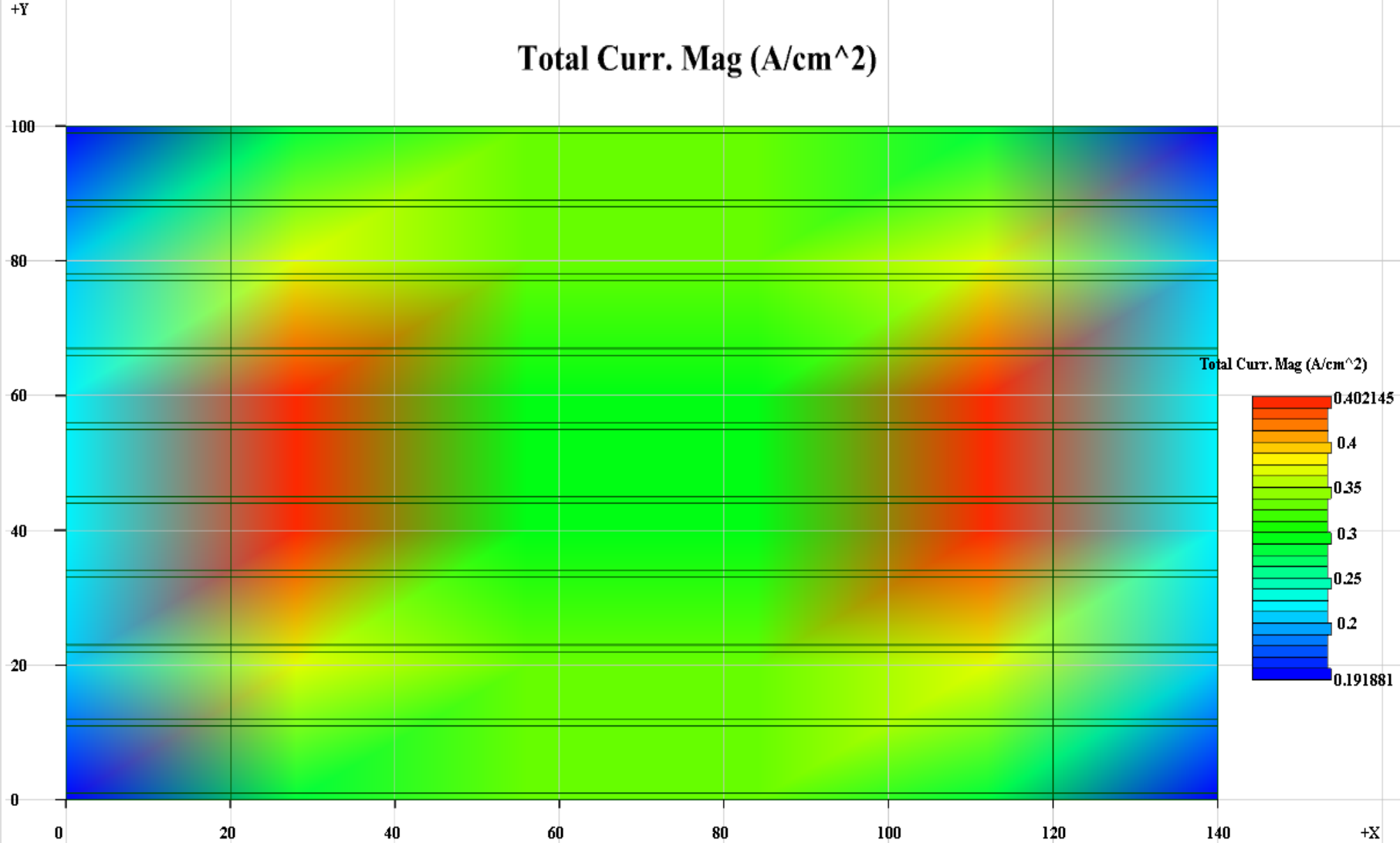


3D current magnitude

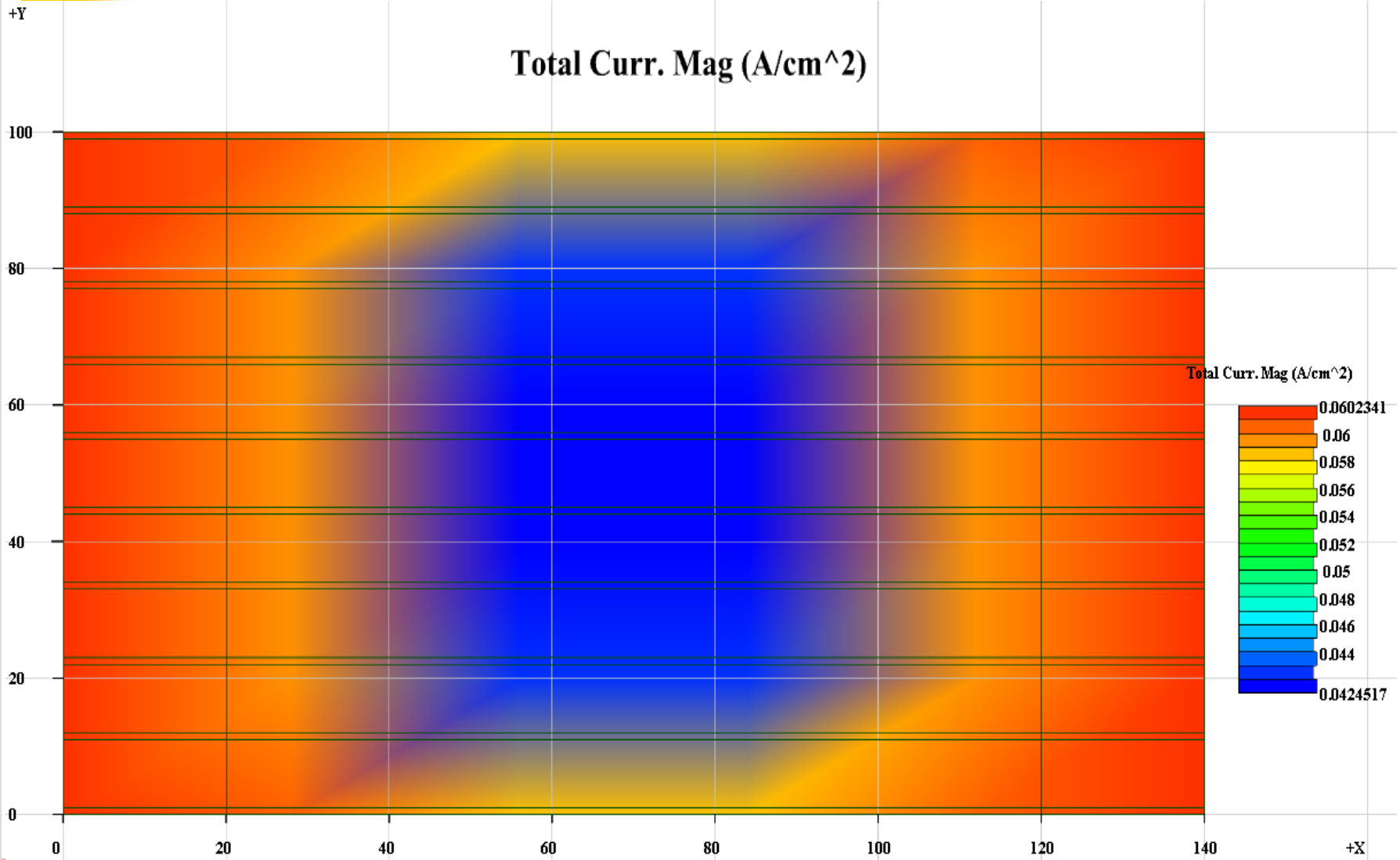


3D current magnitude $y=14$

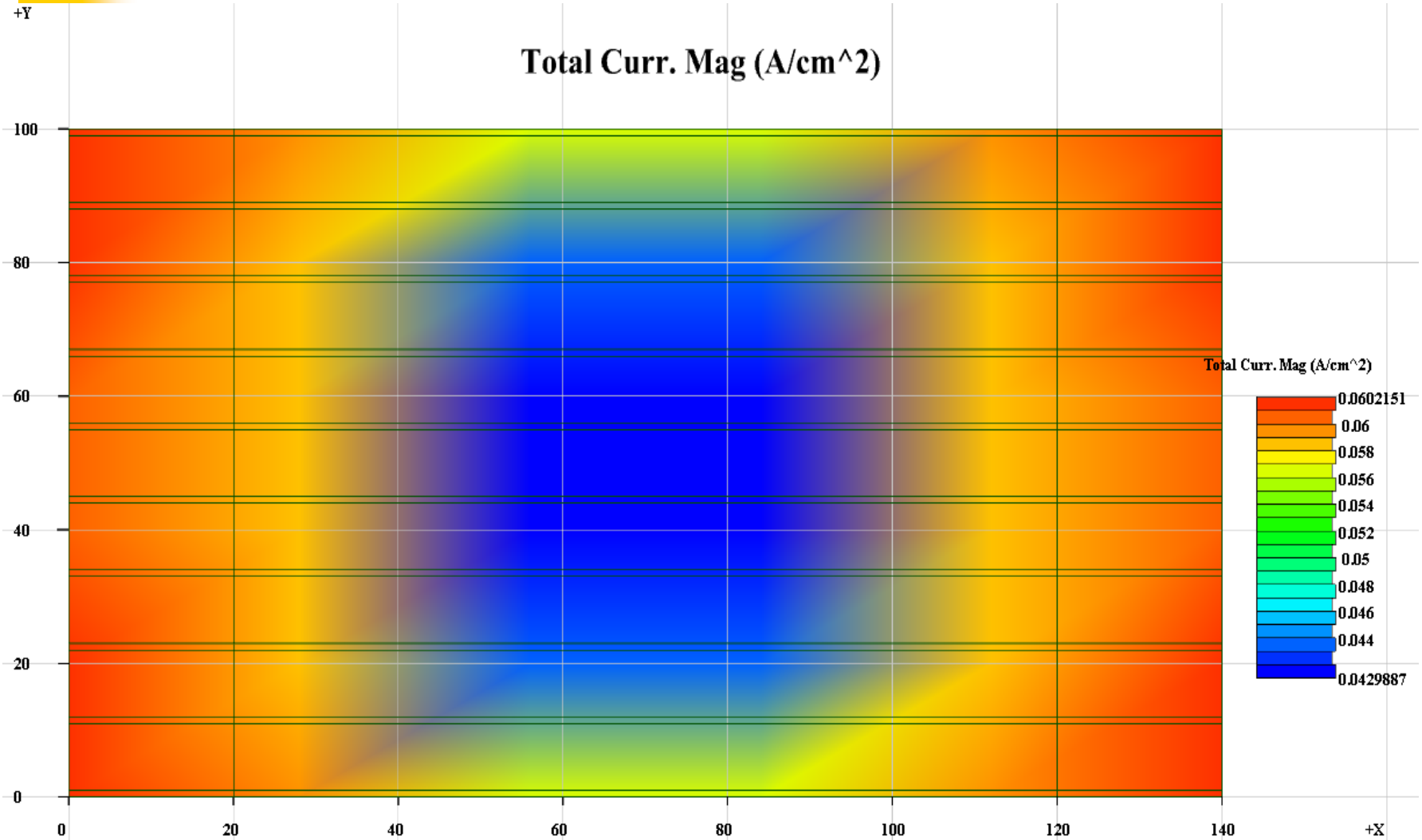
Total Curr. Mag (A/cm²)



3D current magnitude $y=7$

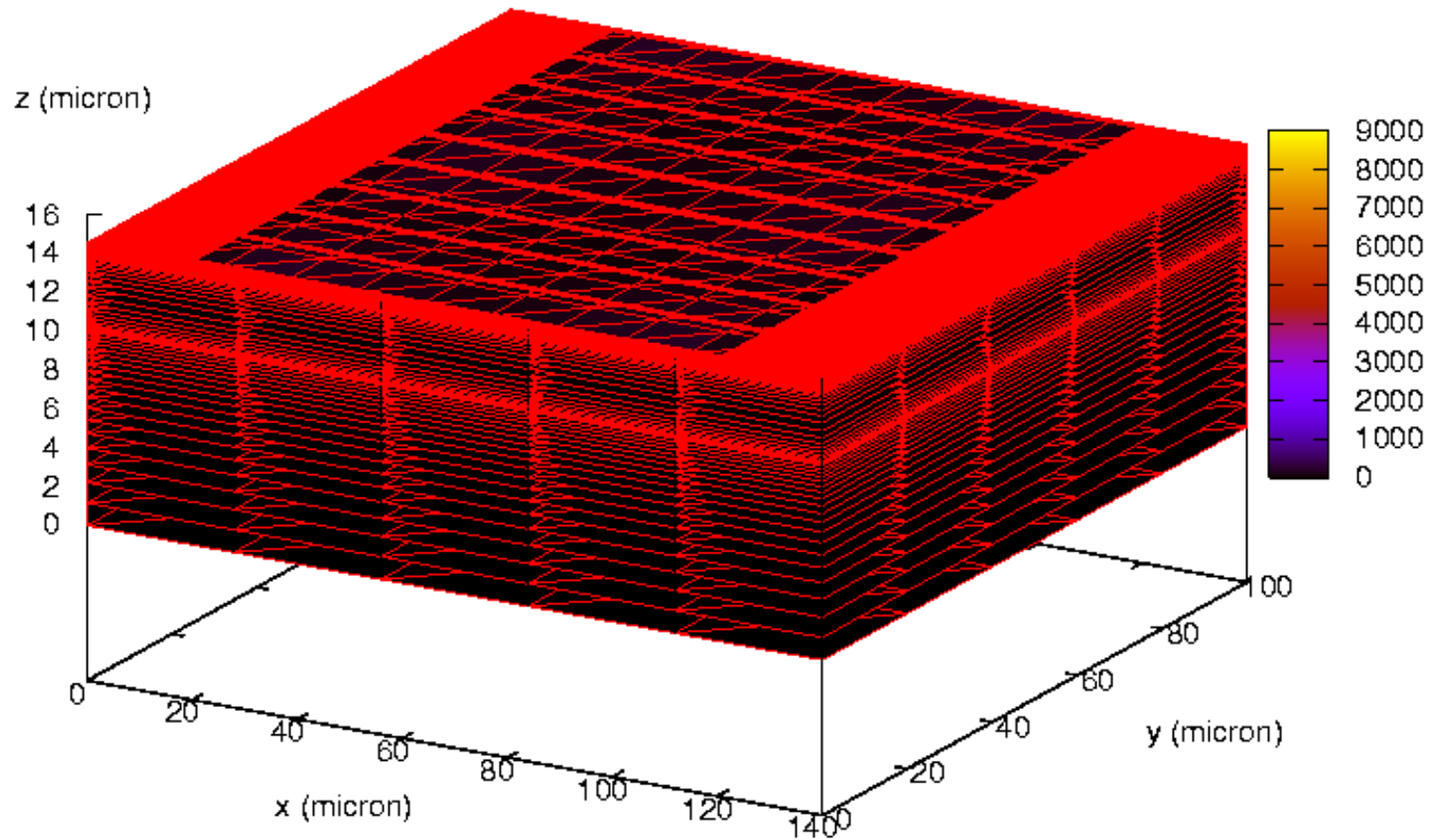


3D current magnitude $y=0$



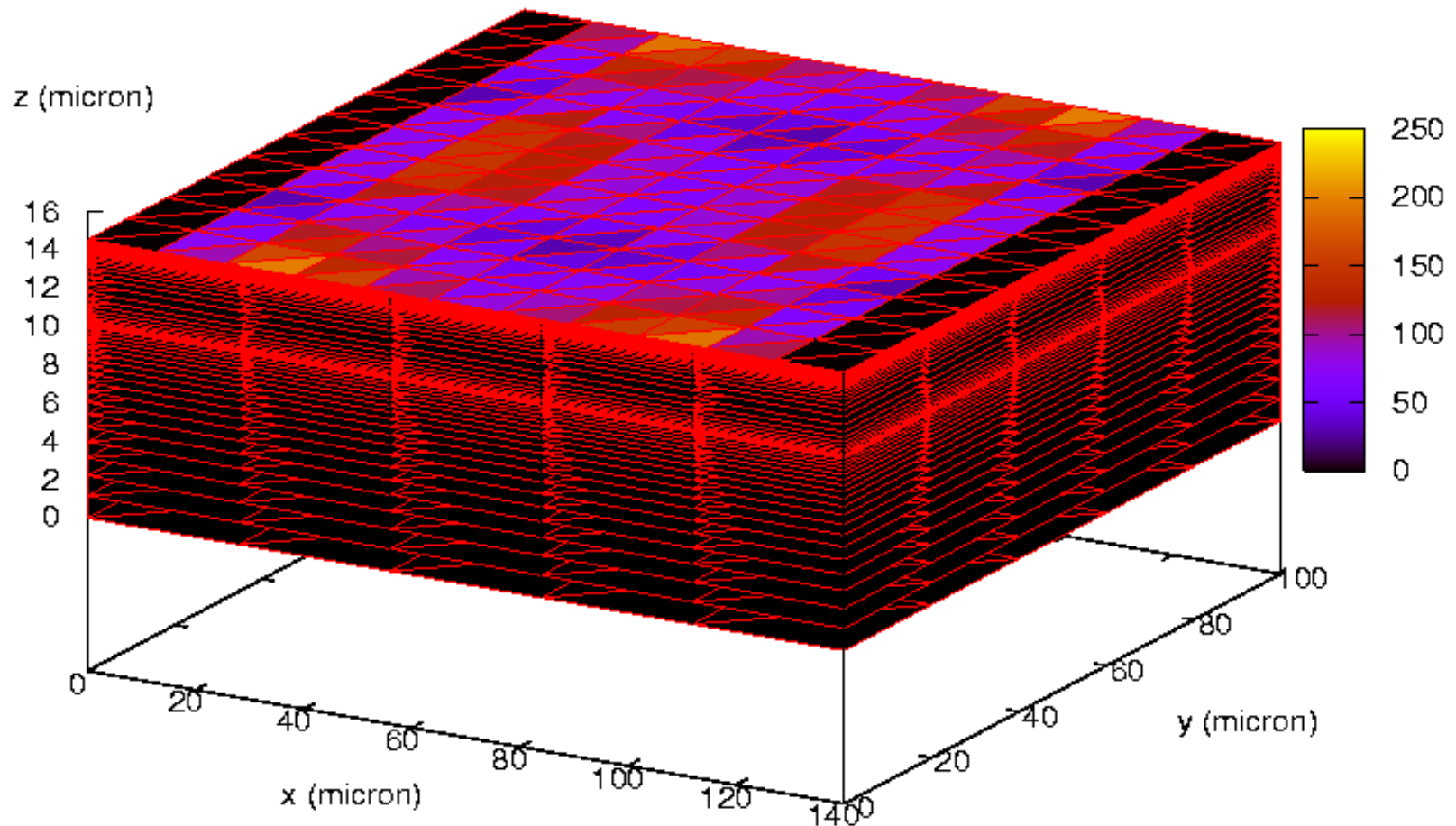
From Plane 1 to Plane 102

Elec. Curr. Mag (A/cm²)

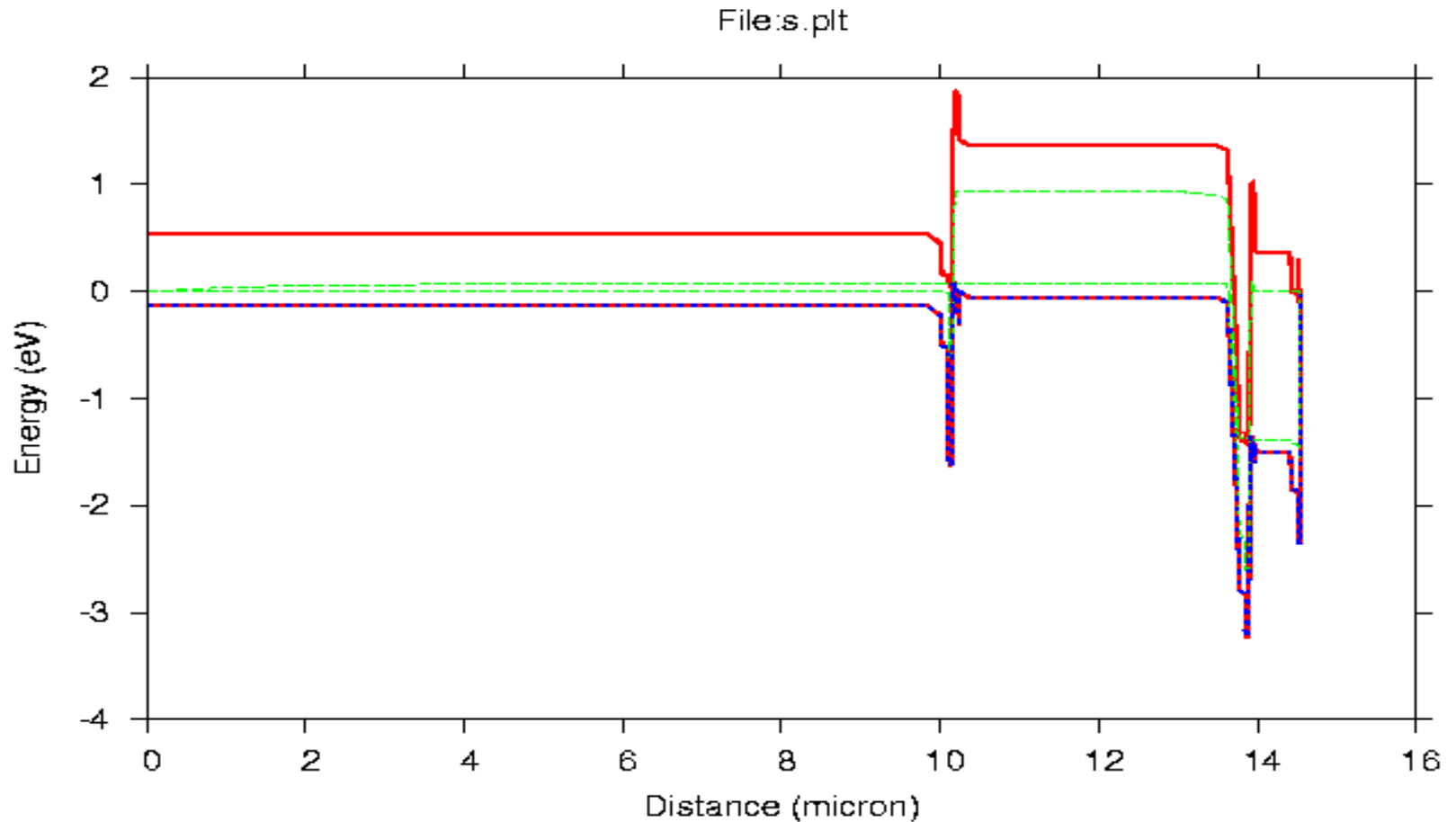


From Plane 1 to Plane 100

Elec. Curr. Mag (A/cm^2)

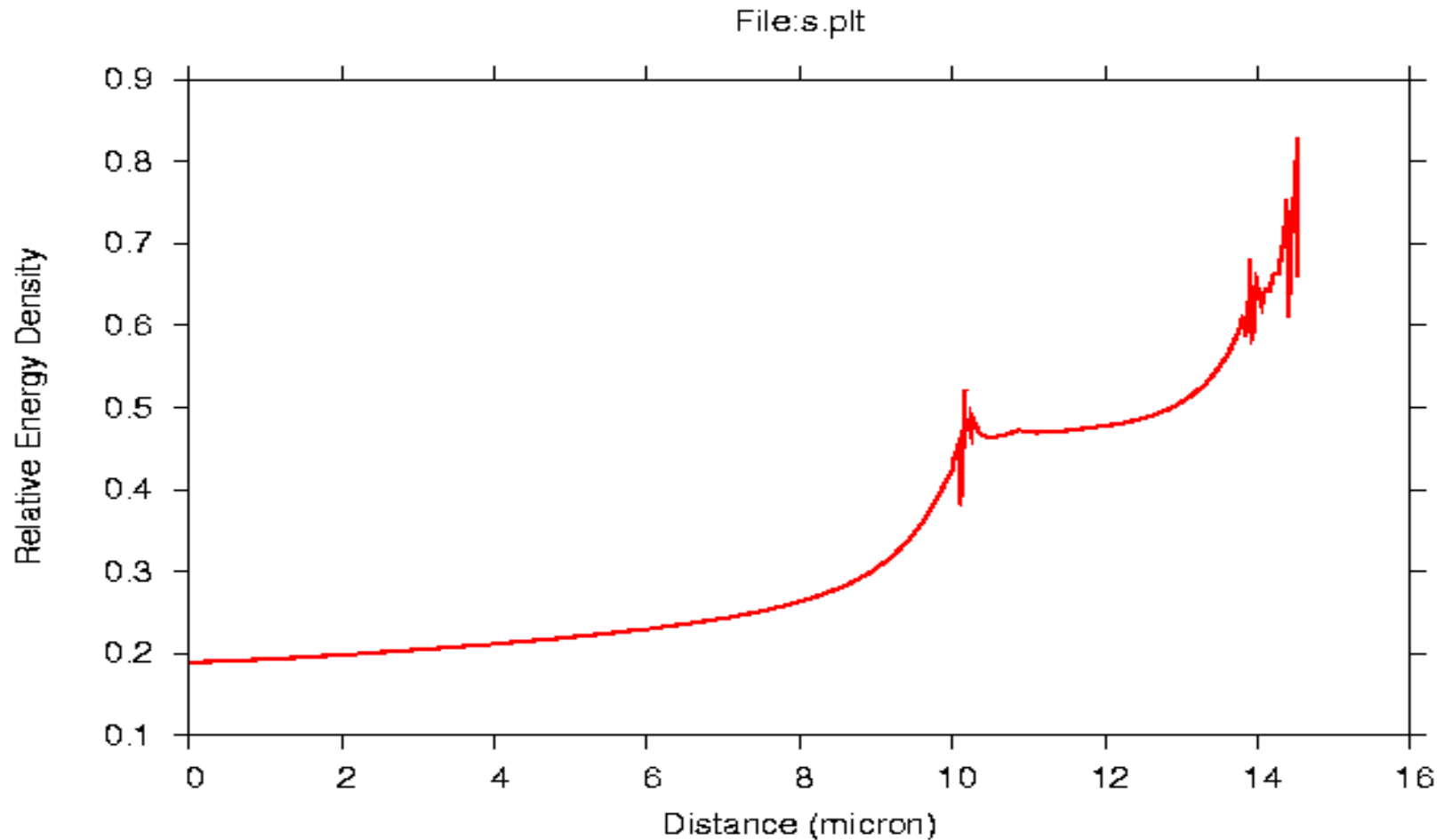


Energy Band Diagram



z-direction

Incident Power at $x=50$ and $y=70$

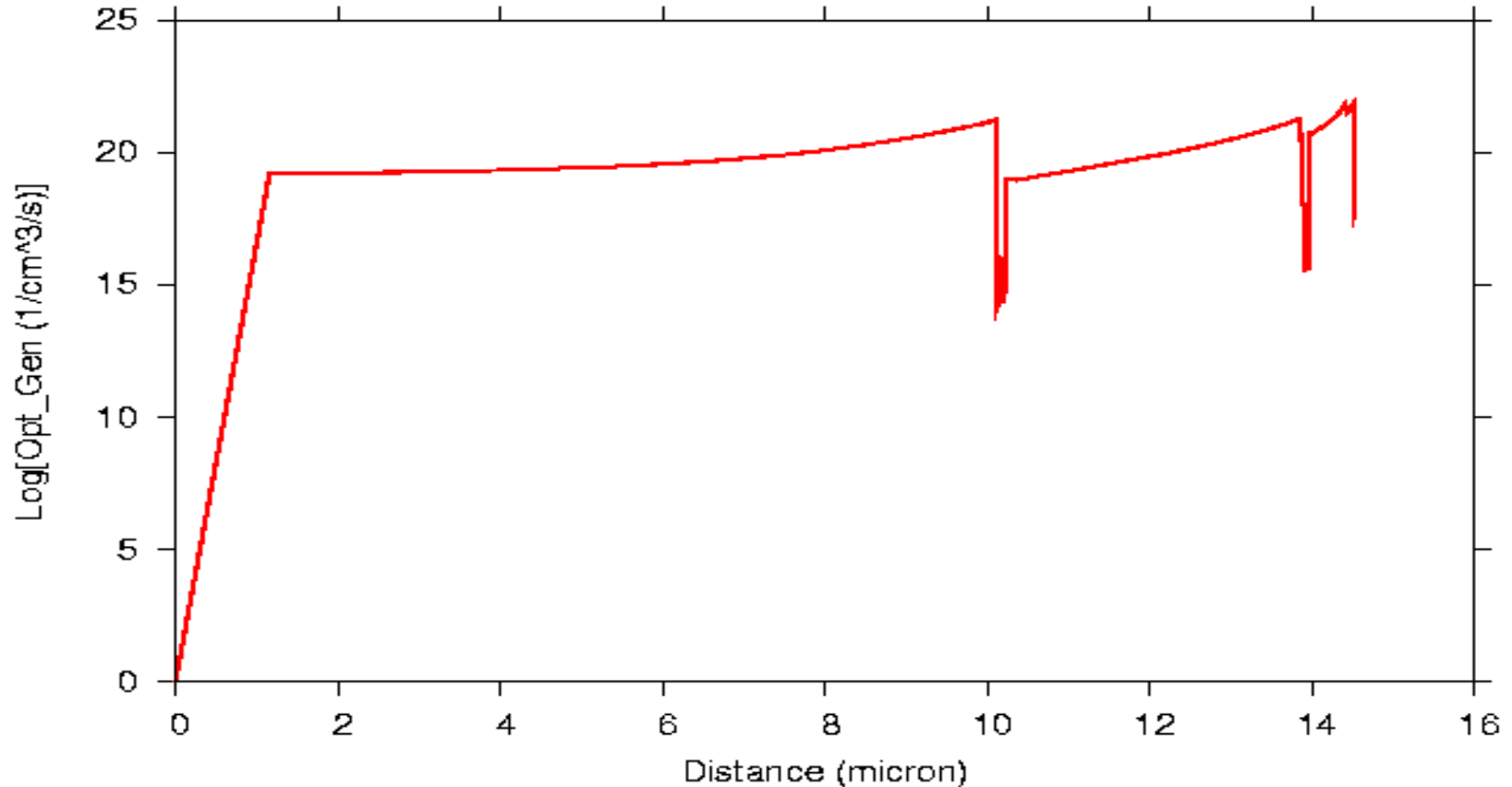


Z-

direction

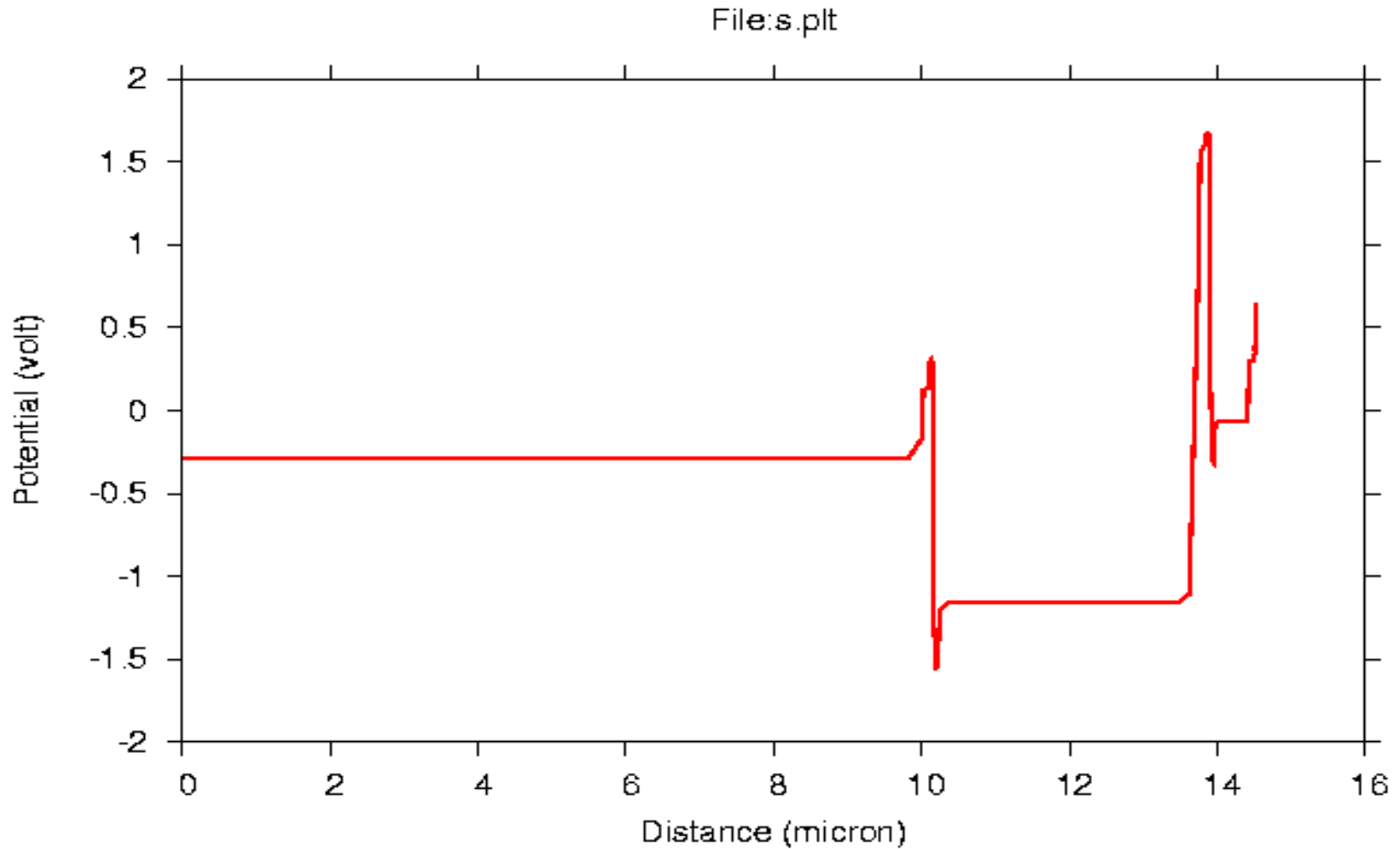
Optical Generation at x=50 and y=70

File:s.plt



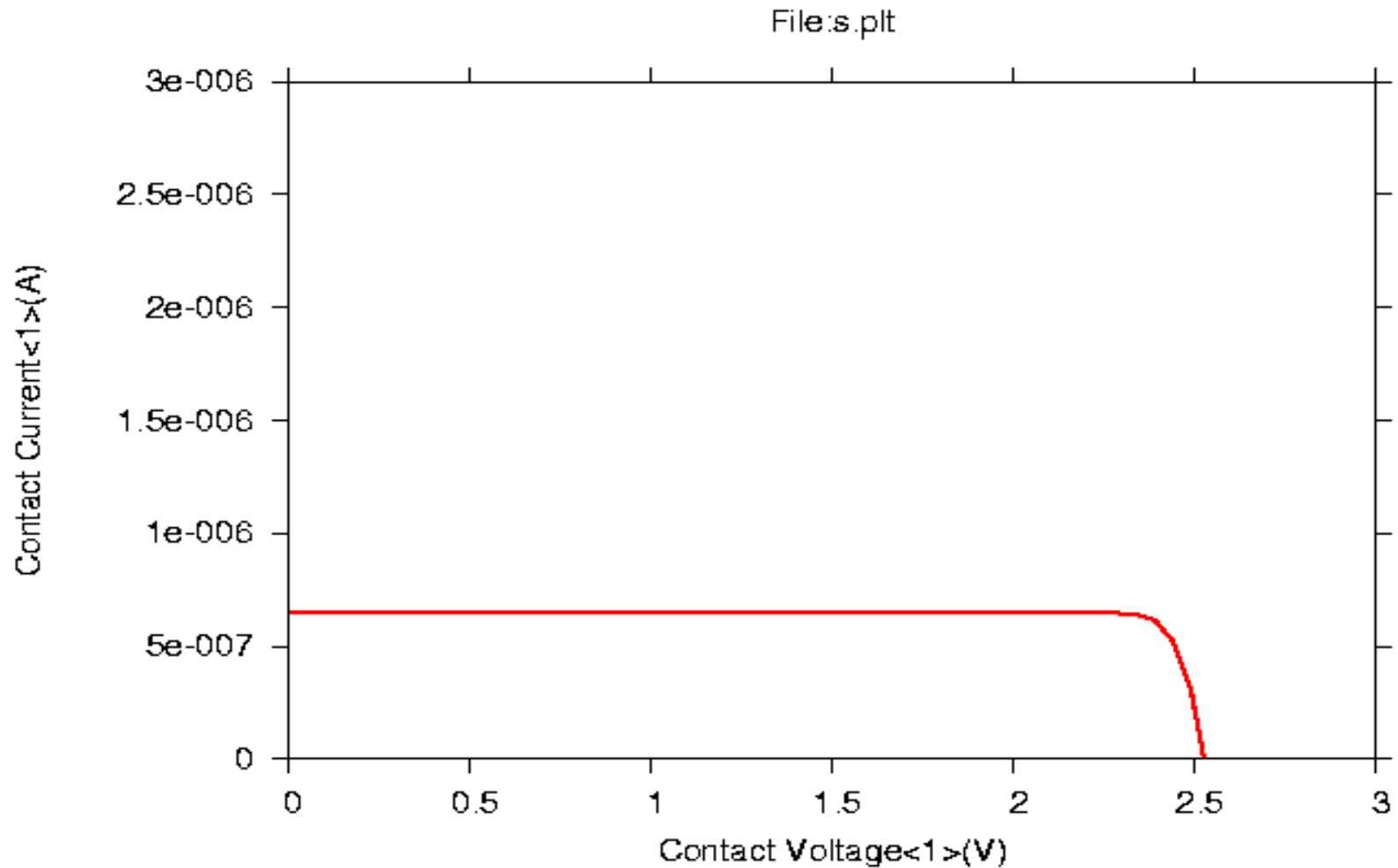
z-
direction

Potential distribution at $x=50$ and $y=70$



Z-
direction

AM1.5 I-V Curve at T=300 K



Conclusion

- ➔ **2D & 3D simulations on compound single and multi-junction solar cells have been demonstrated.**
- ➔ **Non-local tunnel-junction model is calibrated with experiments**
- ➔ **Biased solar spectrum is used to obtain external quantum efficiency.**
- ➔ **Modeling results of I-V curve, I_{sc} , V_{oc} & efficiency consistent with experimental results.**
- ➔ **Modeling results for multi-sun concentration are also presented: optimal sun number varies with contact pad separation, indicating different series resistance effect.**